

1 **Impacts of biogenic polyunsaturated aldehydes on metabolism and community**
2 **composition of particle-attached bacteria in coastal hypoxia**

3 Zhengchao Wu^{1,2}, Qian P. Li^{1,2,3,*}, Zaiming Ge^{1,3}, Bangqin Huang⁴, Chunming Dong⁵

4 ¹State Key Laboratory of Tropical Oceanography, South China Sea Institute of Oceanology, Chinese
5 Academy of Sciences, Guangzhou, China

6 ²Southern Marine Science and Engineering Guangdong Laboratory, Guangzhou, China

7 ³College of Marine Science, University of the Chinese Academy of Sciences, Beijing, China

8 ⁴Fujian Provincial Key Laboratory of Coastal Ecology and Environmental Studies, State Key Laboratory of
9 Marine Environmental Science, Xiamen University, Xiamen, China

10 ⁵Key Laboratory of Marine Genetic Resources, Third Institute of Oceanography, MNR, Xiamen, China

11 *Correspondence to: Qian Li (qianli@scsio.ac.cn)

12

13 **Abstract.** Eutrophication-driven coastal hypoxia is of great interest for decades, though its mechanisms
14 remain not fully understood. Here, we showed elevated concentrations of particulate and dissolved
15 polyunsaturated aldehydes (PUAs) associated with the hypoxic waters in the bottom layer of a salt-wedge
16 estuary. Bacterial respiration within the hypoxic waters was mainly contributed by particle-attached
17 bacteria (PAB) ($>0.8 \mu\text{m}$), with free-living bacteria ($0.2\text{-}0.8 \mu\text{m}$) only accounting for 25-30 % of the total
18 rate. The concentration of particle-adsorbed PUAs ($\sim 10 \mu\text{mol L}^{-1}$) in the hypoxic waters were directly
19 quantified for the first time based on large-volume-filtration and subsequent on-site PUAs derivation and
20 extraction. PUAs-amended incubation experiments for PAB ($>25 \mu\text{m}$) associated with sinking or suspended
21 particles retrieved from the low-oxygen waters were also performed to explore the impacts of PUAs on the
22 growth and metabolism of PAB and associated oxygen utilization. We found an increase in cell growth of
23 PAB in response to low-dose PUAs ($1 \mu\text{mol L}^{-1}$) but an enhanced cell-specific bacterial respiration and
24 production in response to high-dose PUAs ($100 \mu\text{mol L}^{-1}$). Improved cell-specific metabolism of PAB in

25 response to high-dose PUAs was also accompanied by a shift of PAB community structure with increased
26 dominance of genus *Alteromonas* within the Gammaproteobacteria. We thus conclude that a high PUAs
27 concentration associated with aggregate particles within the bottom layer may be crucial for some species
28 within *Alteromonas* to regulate PAB community structure. The change of bacteria community could lead to
29 an enhancement of oxygen utilization during the degradation of particulate organic matters and thus likely
30 contribute to the formation of coastal hypoxia. These findings are potentially important for coastal systems
31 with large river inputs, intense phytoplankton blooms driven by eutrophication, as well as strong hypoxia
32 developed below the salt-wedge front.

33 **1. Introduction**

34 Coastal hypoxia, defined as dissolved oxygen levels $< 62.5 \mu\text{mol kg}^{-1}$, has become a worldwide problem in
35 recent decades (Diaz and Rosenberg, 2008; Helm et al., 2011). It could affect diverse life processes from
36 genes to ecosystems, resulting in the spatial and temporal change of marine food-web structures (Breitburg
37 et al., 2018). Coastal deoxygenation is also tightly coupled with other global issues, such as global warming
38 and ocean acidification (Doney et al., 2012). Formation and maintenance of eutrophication-derived hypoxia
39 in the coastal waters should reflect the interaction between physical and biogeochemical processes (Kemp
40 et al., 2009). Generally, seasonal hypoxia occurs in the coastal ocean when strong oxygen sinks are coupled
41 with restricted resupply during periods of strong density stratification. Termination of the event occurs with
42 oxygen resupply when stratification is eroded by vertical mixing (Fennel and Testa, 2019).

43 Bacterial respiration accounts for the largest portion of aquatic oxygen consumption and is thus pivotal
44 for the development of hypoxia and oxygen minimum zones (Williams and del Giorgio, 2005; Diaz and
45 Rosenberg, 2008). Generally, free-living bacteria (FLB, $0.2\text{-}0.8 \mu\text{m}$) dominate the community respiration in
46 many parts of the ocean (Robinson and Williams, 2005; Kirchman, 2008). Compared to the FLB, the role
47 of particle-attached bacteria (PAB, $>0.8 \mu\text{m}$) on community respiration is less addressed, particularly in the
48 coastal oceans. In some coastal waters, PAB can be more important than the FLB with a higher metabolic
49 activity that might affect carbon cycle through organic matter remineralization (Garneau et al., 2009; Lee et
50 al., 2015). PAB was found more abundant than the FLB with a higher diversity near the mouth of the Pearl
51 River estuary (PRE) (Li et al., 2018; Liu et al., 2020; Zhang et al., 2016). An increased contribution of PAB
52 to respiration relative to FLB can occur during the development of coastal phytoplankton bloom (Huang et
53 al., 2018). In the Columbia River estuary, the particle-attached bacterial activity could be 10-100 folds
54 higher than that of its free-living counterparts leading to its dominant role in organic detritus
55 remineralization (Crump et al., 1998). Therefore, it is crucial to assess the respiration process associated
56 with PAB and its controlling factors in these regions, to fully understand oxygen utilization in the hypoxic
57 area with an intense supply of particulate organic matters.

58 There is an increasing area of seasonal hypoxia in the nearshore bottom waters of the Pearl River
59 Estuary and the adjacent northern South China Sea (NSCS) (Yin et al., 2004; Zhang and Li 2010; Su et al.,
60 2017). The hypoxia is generally developed at the bottom of the salt-wedge where downward mixing of
61 oxygen is restrained due to increased stratification and where there is an accumulation of
62 eutrophication-derived organic matter due to flow convergence driven by local hydrodynamics (Lu et al.,
63 2018). Besides physical and biogeochemical conditions, aerobic respiration is believed the ultimate cause
64 of hypoxia here (Su et al., 2017). Thus, microbial respiration had been strongly related to the consumption
65 of bulk dissolved organic carbon in the PRE hypoxia (He et al., 2014).

66 Phytoplankton-derived polyunsaturated aldehydes (PUAs) are known to affect marine microorganisms
67 over various trophic levels by acting as infochemicals and/or by chemical defenses (Ribalet et al., 2008;
68 Ianora and Miralto, 2010; Edwards et al., 2015; Franzè et al., 2018). PUAs are produced by stressed
69 diatoms during the oxidation of membrane polyunsaturated fatty acids (PUFA) by lipoxygenase (Pohnert
70 2000) and are released from the surface of particles to the seawater by diffusion. A perennial bloom of
71 PUA-producing diatoms near the mouth of the PRE (Wu and Li, 2016) should support the importance of
72 PUAs relative to other phytoplankton-derived organic compounds, such as karlotoxin by dinoflagellates,
73 cyanotoxin by cyanobacteria, and dimethylsulphoniopropionate mainly by prymnesiophytes. Besides PUAs,
74 there are other signaling molecules that may potentially affect bacterial activities in the low oxygen waters,
75 such as 2-n-pentyl-4-quinolinol (PQ) and acylated homoserine lactones (AHL). PQ could be less important
76 here in terms of hypoxia formation as it is generally produced as antibiosis by PAB such as *Alteromonas sp.*
77 to inhibit respirations of other PAB (Long et al., 2003). AHL could also play a less important role here since
78 the AHL-mediated quorum-sensing could be constrained by a large pH fluctuation from 7.2 to 8.8 in the
79 bottom waters of the PRE (Decho et al., 2009).

80 The level of PUAs in the water-column are inhomogeneous, varying from sub-nanomolar offshore to
81 nanomolar nearshore (Vidoudez et al., 2011; Wu and Li, 2016; Bartual et al., 2018), and to micromolar
82 associated with particle hotspots (Edwards et al., 2015). The strong effect of PUAs on bacterial growth,

83 production, and respiration has been well demonstrated in laboratory studies (Ribalet et al., 2008) and field
84 studies (Balestra et al., 2011; Edwards et al., 2015). A nanomolar level of PUAs recently reported in the
85 coastal waters outside the PRE was hypothesized to affect oxygen depletion by promoting microbial
86 utilization of organic matters in the bottom waters (Wu and Li, 2016). Meanwhile, the actual role of PUAs
87 on bacterial metabolism within the bottom hypoxia remains largely unexplored.

88 In this study, we investigate the particle-attached bacteria within the core of the hypoxic waters by
89 exploring the linkage between PUAs and bacterial oxygen utilization on the suspended organic particles.
90 There are three specific questions to address here: What are the relative roles of PAB and FLB on bacterial
91 respiration in the hypoxic waters? What are the actual levels of PUAs in the hypoxic waters? What are the
92 responses of PAB to PUAs in the hypoxic waters? For the first question, size-fractionated bacterial
93 respiration rates were estimated for both FLB (0.2-0.8 μm) and PAB ($>0.8 \mu\text{m}$) in the hypoxic waters. For
94 the second question, the concentrations of particulate and dissolved PUAs within the hypoxic waters were
95 measured in the field. Besides, the hotspot PUAs concentration associated with the suspended particles
96 within the hypoxic waters was directly quantified for the first time using large-volume filtration and
97 subsequent on-site derivation and extraction. For the third question, field PUAs-amended incubation
98 experiments were conducted for PAB ($>25 \mu\text{m}$) retrieved from the low-oxygen waters. We focused on
99 particles of $>25 \mu\text{m}$ to better explore the role of PUAs on PAB associated with sinking or suspended
100 particles. The doses of PUAs treatments were selected to represent the actual levels of PUAs hotspots, to
101 assess the PAB responses (including bacterial abundance, respiration, production, and community
102 composition) to the exogenous PUAs in the hypoxic waters. By synthesizing these experimental results
103 with the change of water-column biogeochemistry, we hope to explore the underlying mechanism for
104 particle-adsorbed PUAs influencing on community structure and metabolism of PAB in the low-oxygen
105 waters, as well as to understand its contribution to coastal deoxygenation of the NSCS shelf-sea.

106

107 **2. Methods**

108 **2.1 Descriptions of field campaigns and sampling approaches**

109 Field survey cruises were conducted in the PRE and the adjacent NSCS during June 17th-28th, 2016 and
110 June 18st-July 2nd, 2019 (Figure 1). Briefly, vertical profiles of temperature, salinity, dissolved oxygen, and
111 turbidity were acquired from a Seabird 911 rosette sampling system. The oxygen sensor data were corrected
112 by field titration measurements during the cruise. Water samples at various depths were collected using 6 or
113 12 liters (12 or 24 positions) Niskin bottles attached to the Rosette sampler. Surface water samples were
114 collected at ~1m or 5 m depth, while bottom water samples were obtained at depths ~4 m above the bottom.
115 Chlorophyll-*a* (Chl-*a*) samples were taken at all depths at all stations and nutrients were also sampled
116 except at a few discrete stations. For the 2016 cruise, samples for pPUAs were collected at all depths close
117 to station X1 (Figure 1A). During the summer of 2019, vertical profiles of particulate PUAs (pPUAs) and
118 dissolved PUAs (dPUAs) were determined at Y1 in the hypoxic zone and Y2 outside the hypoxic zone with
119 field PUAs-amended experiments conducted at Y1 (Figure 1B). For station Y1, the middle layer was
120 defined as 12 m with the bottom layer as 25 m. At this station, samples at different depths were collected
121 for determining the size-fractionated respiration rates and the whole water bacterial taxonomy.

123 **2.2 Determination of chlorophyll-*a*, dissolved nutrients**

124 For Chl-*a* analyses, 500 mL of water sample was gently filtered through a 0.7 μm Whatman GF/F filter.
125 The filter was then wrapped by a piece of aluminum foil and stored at -20 °C on board. Chl-*a* was extracted
126 at 4 °C in the dark for 24 h using 5 mL of 90% acetone. After centrifuged at 4000 rpm for 10 min, Chl-*a*
127 was measured using a standard fluorometric method with a Turner Designs fluorometer (Parsons et al.,
128 1984). Water samples for nutrients were filtered through 0.45 μm Nucleopore filters and stored at -20 °C.
129 Nutrient concentrations including nitrate plus nitrite, phosphate, and silicate were measured using a
130 segmented-flow nutrient autoanalyzer (Seal AA3, Bran-Luebbe, GmbH).

132 **2.3 Sampling and measurements of particulate and dissolved PUAs in one-liter seawater**

133 We used a similar protocol of Wu and Li (2016) for pPUAs and dPUAs collection, pretreatment, and
134 determination. Briefly, 2-4 liters of water sample went through a GF/C filtration with both the filter and the
135 filtrate collected separately. The filter was rinsed by the derivative solution with the suspended particle
136 samples collected in a glass vial. After adding internal standard, the samples in the vial were frozen and
137 thawed three times to mechanically break the cells for pPUAs. The filtrate from the GF/C filtration was
138 also added with internal standard and transferred to a C18 solid-phase extraction cartridge. The elute from
139 the cartridge with the derivative solution was saved in a glass vial for dPUAs. Both pPUAs and dPUAs
140 samples were frozen and stored at -20 °C.

141 In the laboratory, the pPUAs sample was thawed with the organic phase extracted. After the solvent
142 was evaporated with the sample concentrated and re-dissolved in hexane, pPUAs was determined using gas
143 chromatography and mass spectrometry (Agilent Technologies Inc., USA). Standards series were prepared
144 by adding certain amounts of three major PUAs to the derivative solution and went through the same
145 pretreatment and extraction steps as samples. Derivatives of dPUAs were extracted and measured by
146 similar methods as pPUAs, except that the calibration curves of dPUAs were constructed separately. The
147 units of pPUAs and dPUAs are nmol L^{-1} (nmol PUA in one-liter seawater).

148

149 **2.4 Particle collections by large-volume filtrations in hypoxia waters.**

150 Large volumes (~300 L) of the middle (12 m) and the bottom (25 m) waters within the hypoxia zone were
151 collected by Niskin bottles at station Y1. For each layer, the water sample was quickly filtered through a
152 sterile fabric screen (25 μm filter) on a disk filter equipped with a peristaltic pump to qualitatively obtain
153 particles of $>25 \mu\text{m}$. Larger zooplankters were picked off immediately. The particle samples were gently
154 back-flushed three times off the fabric screen using particle-free seawater (obtained using a 0.2 μm
155 filtration of the same local seawater) into a sterile 50-mL sampling tube.

156 The volume of total particles from large-volume-filtration was measured as follows: The collected
157 particle in the 50 mL tube was centrifuged for one minute at a speed of 3000 revolutions per minute (r.p.m)

158 with the supernatant saved (Hmelo et al., 2011). The particle sample was resuspended as slurry by gently
159 shaking and transferred into a sterile 5 mL graduated centrifuge tube. The sample was centrifuged again by
160 the same centrifuging speed with the final volume of the total particles recorded. The unit for the total
161 particle volume is mL.

162 All the particles were transferred back to the sterile 50 mL centrifuge tube (so as all the supernatants)
163 with 0.2- μ m-filtered seawater, which was used for subsequent measurements of particle-adsorbed PUAs as
164 well as for PUAs-amended incubation experiments of particle-attached bacteria.

165

166 **2.5 Measurements of particle-adsorbed PUAs**

167 After gently shaking, 3 mL of sample in the 50 mL sampling tube (see section 2.4) was used for the
168 analyses of particle-adsorbed PUAs concentration (two replicates) according to the procedure shown in
169 Figure 2 (modified from the protocols of Edwards et al. 2015 and Wu and Li 2016). The sample (3 mL) was
170 transferred to 50 mL centrifuge tubes for PUAs derivatization on board. An internal standard of
171 benzaldehyde was added to obtain a final concentration of 10 μ M. The aldehydes in the samples were
172 derivatized by the addition of O-(2,3,4,5,6-pentafluorobenzyl) hydroxylamine hydrochloride solution in
173 deionized water ($pH=7.5$). The reaction was performed at room temperature for 15 min (shaking slightly
174 for mix every 5 min). Then 2 mL sulfuric acid (0.1%) solution was added to a final concentration of 0.01%
175 acid (pH of 2-3) to avoid new PUAs induced by enzymatic cascade reactions. The derivate samples were
176 subsequently sonicated for 3 min before the addition of 20 mL hexane, and the upper organic phase of the
177 extraction was transferred to a clean tube and stored at -20 $^{\circ}$ C.

178 Upon returning to the laboratory, the adsorbed PUAs on these particles (undisrupted PUAs) were
179 determined with the same analytical methods as those for the disrupted pPUAs (freeze-thaw methods to
180 include the portion of PUAs eventually produced as cells die, Wu and Li 2016) except for the freeze-thaw
181 step. A separate calibration curve was made for the undisrupted PUAs derivates. A standard series of
182 heptadienal, octadienal, and decadienal (0, 0.1, 0.5, 1.0, 2.5, 5.0, 10.0, 25.0 nmol L^{-1}) was prepared before

183 each analysis by diluting a relevant amount of the PUA stock solution (methanolic solution) with deionized
184 water. These standard solutions were processed through all the same experimental steps as those mentioned
185 above for derivation, extraction, and measurement of the undisrupted PUAs sample. The unit for the
186 undisrupted PUAs is nmol L^{-1} . The total amount of the undisrupted PUAs in the 50 mL sampling tube was
187 the product of the measured concentration and the total volume of the sample.

188 The hotspot PUAs concentration associated with the aggregate particles is defined as the PUAs
189 concentration in the volume of the water parcel displaced by these particles. Therefore, the final
190 concentration of particle-adsorbed PUAs in the water column, defined as PUAs [$\mu\text{mol L}^{-1}$], should be equal
191 to the moles of particle-adsorbed PUAs (nmol, the undisrupted PUAs) divided by the volume of particles
192 (mL).

193

194 **2.6 Incubation of particle-attached bacteria with PUAs treatments.**

195 The impact of PUAs on microbial growth and metabolisms in the hypoxia zone was assessed by field
196 incubation of particle-attached bacteria on particles of $> 25 \mu\text{m}$ collected from large-volume filtration with
197 direct additions of low or high doses of PUAs (1 or $100 \mu\text{mol L}^{-1}$) on June, 29th, 2019 (Figure 2).

198 A sample volume of $\sim 32 \text{ mL}$ in the centrifuge tube (section 2.4) was transferred to a sterile Nalgene
199 bottle before being diluted by particle-free seawater to a final volume of 4 L. About 3.2 L of the sample
200 solution was transferred into four sterile 1-L Nalgene bottles (each with 800 mL). One 1-L bottle was used
201 for determining the initial conditions: after gentle shaking, the solution was transferred into six biological
202 oxygen demand (BOD) bottles with three for initial oxygen concentration (fixed immediately by Winkler
203 reagents) and the other three for initial bacterial abundance, production, and community structure. The
204 other three 1-L bottles were used for three different treatments (each with two replicates in two 0.5-L
205 bottles): the first one served as the control with the addition of 200 μL methanol, the second one with 200
206 μL low-dose PUAs solution, and the third one with 200 μL high-dose PUAs solution (Table 1). The
207 solution in each of the three treatments (0.5L bottles) was transferred to six parallel replicates by 60-mL

208 BOD bottles. These BOD bottles were incubated at *in situ* temperature in the dark for 12 hours. At the end
209 of each incubation experiment, three of the six BOD bottles were used for determining the final oxygen
210 concentrations with the other three for the final bacterial abundance, production, and community structure.

211 To test the possibility of PUAs as carbon sources for bacterial utilization, a minimal medium was
212 prepared with only sterile artificial seawater but not any organic carbons (Dyksterhouse et al., 1995). A
213 volume of 375 μL sample (from the above 4 L sample solution) was inoculated in the minimal medium
214 amended with heptadienal in a final concentration of about 200 $\mu\text{mol L}^{-1}$. This PUA level was close to the
215 hotspot PUAs of 240 $\mu\text{mol L}^{-1}$ found in the suspended particles of a station near the PRE. It was also
216 comparable to the hotspot PUAs of 25.7 $\mu\text{mol L}^{-1}$ in the temperate west North Atlantic (Edwards et al.,
217 2015). For comparisons, the same amount of sample was also inoculated in the minimal medium (75 mL)
218 amended with an alkane mixture (ALK, n-pentadecane and n-heptadecane) at a final concentration of 0.25
219 g L^{-1} , or with a mixture of polycyclic aromatic hydrocarbons (PAH, naphthalene and phenanthrene) at a
220 final concentration of 200 ppm. These experiments were performed in dark at room temperature for over 30
221 days. Significant turbidity changes in the cell culture bottle over incubation time will be observed if there is
222 a carbon source for bacterial growth.

223

224 **2.7 Measurements of bacteria-related parameters**

225 **(1) Bacterial abundance**

226 At the end of the 12-h incubation period, a 2 mL sample from each BOD bottle was preserved in 0.5%
227 glutaraldehyde. The fixation lasted for half of an hour at room temperature before being frozen in liquid N_2
228 and stored in a $-80\text{ }^\circ\text{C}$ freezer. In the laboratory, the samples were performed through a previously
229 published procedure for detaching particle-attached bacteria (Lunau et al., 2005), which had been proved
230 effective for samples with high particle concentrations. To break up particles and attached bacteria, 0.2 mL
231 pure methanol was added to the 2 mL sample and vortexed. The sample was then incubated in an ultrasonic
232 bath (35 kHz, 2 x 320W per period) at 35 $^\circ\text{C}$ for 15 min. Subsequently, the tube sample was filtered with a

233 50 μm -filter to remove large detrital particles. The filtrate samples for surface-associated bacteria cells
234 were diluted by 5-10 folds using TE buffer solution and stained with 0.01% SYBR Green I in the dark at
235 room temperature for 40 min. With the addition of 1- μm beads, bacterial abundance (BA) of the samples
236 was counted by a flow cytometer (Beckman Coulter CytoFlex S) with bacteria detected on a plot of green
237 fluorescence versus side scatter (Marie et al., 1997). The precision of the method estimated by the
238 coefficient of variation (CV%) was generally less than 5%.

239 For bulk-water bacteria abundance, 1.8 mL of seawater sample was collected after a 20- μm
240 prefiltration. The sample was transferred to a 2 mL centrifuge tube and fixed by adding 20 μL of 20%
241 paraformaldehyde before storage in a $-80\text{ }^{\circ}\text{C}$ freezer. In the laboratory, 300 μL of the sample after thawing
242 was used for staining with SYBR Green and analyzed using the same flow cytometry method as above
243 (Marie, et al, 1997).

244

245 **(2) Bacterial respiration**

246 For BOD samples, bacterial respiration (BR) was calculated based on the oxygen decline during the 12-h
247 incubation and was converted to carbon units with the respiratory quotient assumed equal to 1 (Hopkinson,
248 1985). Dissolved oxygen was determined by a high-precision Winkler titration apparatus (Metrohm-848,
249 Switzerland) based on the classic method (Oudot et al., 1988). We should mention that BR could be
250 overestimated if phytoplankton and microzooplankton were present in the particle aggregates of $> 25\text{ }\mu\text{m}$.
251 However, this effect could be relatively small because the raw seawater in the hypoxic zone had very low
252 chlorophyll-*a* and because there was virtually not much microzooplankton in the sample (confirmed by
253 FlowCAM).

254 Method for the estimation of the bulk water bacterial respiration at stations X1, X2, and X3 can be
255 found in Xu et al (2018). For the bulk water at station Y1, the size-fractionated respiration rates, including
256 free-living bacteria of 0.2-0.8 μm and particle-associated community of $>0.8\text{ }\mu\text{m}$ (we assumed that they
257 were mostly PAB given the low phytoplankton chlorophyll-*a* of the sample and the absence of zooplankton

258 during the filtration), were estimated based on the method of García-Martín et al (2019). Four 100 mL
259 polypropylene bottles were filled with seawater. One bottle was immediately fixed by formaldehyde. After
260 15 min, the sample in each bottle was incubated in the dark at the *in situ* temperature after the addition of
261 the Iodo-Nitro-Tetrazolium (INT) salt at a final concentration of 0.8 mmol L⁻¹. The incubation reaction
262 lasted for 1.5 h before being stopped by formaldehyde. After 15 min, all the samples were sequentially
263 filtered through 0.8 and 0.2 µm pore size polycarbonate filters and stored frozen until further measurements
264 by spectrophotometry.

265

266 **(3) Bacterial production**

267 Bacterial production (BP) was determined using a modified protocol of the ³H-leucine incorporation
268 method (Kirchman, 1993). Four 1.8-mL aliquots of the sample were collected by pipet from each BOD
269 incubation and added to 2-mL sterile microcentrifuge tubes, which were incubated with ³H-leucine (in a
270 final concentration of 4.65 µmol Leu L⁻¹, Perkin Elmer, USA). One tube served as the control was fixed by
271 adding 100% trichloroacetic acid (TCA) immediately (in a final concentration of 5%). The other three were
272 terminated with TCA at the end of the 2-h dark incubation. Samples were filtered onto 0.2-µm
273 polycarbonate filters and then rinsed twice with 5% TCA and three times with 80% ethanol (Huang et al.,
274 2018) before being stored at -80 °C. In the laboratory, the filters were transferred to scintillation vials with
275 5 mL of Ultima Gold scintillation cocktail. The incorporated ³H was determined using a Tri-Carb 2800TR
276 liquid scintillation counter. Bacterial production was calculated with the previous published
277 leucine-to-carbon empirical conversion factors of 0.37 kg C mol leucine⁻¹ in the study area (Wang et al.,
278 2014). Bacterial carbon demand (BCD) was calculated as the sum of BP and BR. Bacterial growth
279 efficiency (BGE) was equated to BP/BCD.

280

281 **(4) Bacterial community structure**

282 At the end of incubation, the DNA sample was obtained by filtering 30 mL of each BOD water via a
283 0.22- μ m Millipore filter, which was preserved in a cryovial with the DNA protector buffer and stored at
284 -80 °C. DNA was extracted using the DNeasy PowerWater Kit with genomic amplification by Polymerase
285 Chain Reaction (PCR). The V3 and V4 fragments of bacterial 16S rRNA were amplified at 94 °C for 2 min
286 and followed by 27 cycles of amplification (94 °C for 30 s, 55° C for 30 s, and 72 °C for 60 s) before a
287 final step of 72 °C for 10 min. Primers for amplification included 341F (CCTACGGGNGGCWGCAG) and
288 805R (GACTACHVGGGTATCTAATCC). Reactions were performed in a 10- μ L mixture containing 1 μ L
289 Toptaq Buffer, 0.8 μ L dNTPs, 10 μ M primers, 0.2 μ L Taq DNA polymerase, and 1 μ L Template DNA.
290 Three parallel amplification products for each sample were purified by an equal volume of AMpure XP
291 magnetic beads. Sample libraries were pooled in equimolar and paired-end sequenced (2 \times 250 bp) on an
292 Illumina MiSeq platform.

293 High-quality sequencing data was obtained by filtering on the original off-line data. Briefly, the raw
294 data was pre-processed using TrimGalore to remove reads with qualities of less than 20 and FLASH2 to
295 merge paired-end reads. Besides, the data were also processed using Usearch to remove reads with a total
296 base error rate of greater than 2 and short reads with a length of less than 100 bp and using Mothur to
297 remove reads containing more than 6 bp of N bases. We further used UPARSE to remove the singleton
298 sequence to reduce the redundant calculation during the data processing. Sequences with similarity greater
299 than 97% were clustered into the same operational taxonomic units (OTUs). R software was used for
300 community composition analysis.

301 DNA samples for the bulk bacteria (>0.2 μ m) and PAB on particles of > 25 μ m at station Y1 were also
302 collected for bacterial community analysis using the same method described above. Methods for the bulk
303 water bacterial community analyses at stations X1, X2, and X3 during the 2016 cruise can be found in the
304 published paper of Xu et al. (2018).

305

306 **2.8 Statistical Analysis**

307 All statistical analyses were performed using the statistical software SPSS (Version 13.0, SPSS Inc.,
308 Chicago, IL, USA). A student's t-test with a 2-tailed hypothesis was used when comparing PUAs-amended
309 treatments with the control or comparing stations inside and outside the hypoxic zone, with the null
310 hypothesis being rejected if the probability (p) is less than 0.05. We consider p of <0.05 as significant and p
311 of <0.01 as strong significant. Ocean Data View with the extrapolation model "DIVA Gridding" method
312 was used to contour the spatial distributions of physical and biogeochemical parameters.

313

314 **3. Results**

315 **3.1 Characteristics of hydrography, biogeochemistry, and bulk bacteria community in the hypoxic** 316 **zone**

317 During our study periods, there was a large body of low oxygen bottom water with the strongest hypoxia ($<$
318 $62.5 \mu\text{mol kg}^{-1}$) on the western shelf of the PRE (Figure 1), which was relatively similar among different
319 summers of 2016 and 2019 (Figure 1). For vertical distribution, a strong salt-wedge structure was found
320 over the inner shelf (Figures 3A, 3D) with freshwater on the shore side due to intense river discharge.
321 Bottom waters with oxygen deficiency ($< 93.5 \mu\text{mol kg}^{-1}$) occurred below the lower boundary of the
322 salt-wedge and expanded ~ 60 km offshore (Figure 3E). In contrast, a surface high Chl- a patch ($6.3 \mu\text{g L}^{-1}$)
323 showed up near the upper boundary of the front, where there was enhanced water-column stability, low
324 turbidity, and high nutrients (Figures 3B, 3C). Therefore, there was a spatial mismatch between the
325 subsurface hypoxic zone (Figure 3E) and the surface chlorophyll-bloom (Figure 3F) during the
326 estuary-to-shelf transect, as both the surface Chl- a and oxygen right above the hypoxic zones at the bottom
327 boundary of the salt-wedge were not themselves maxima.

328 There were much higher rates of respiration (BR) ($t=7.8$, $n=9$, $p<0.01$) and production (BP) ($t=13.0$,
329 $n=9$, $p<0.01$) for the bulk bacterial community (including FLB and PAB) in the bottom waters of X1 within
330 the hypoxic core than those of X2 and X3 outside the hypoxic zone during June 2016 (Figure 4, modified
331 from data of Xu et al., 2018). The size-fractionated respiration rates were quantified at station Y1 during the

2019 cruise (Figure S1) to distinguish the different roles of FLB and PAB on bacterial respiration in the hypoxic waters. Our results suggested that bacterial respiration within the hypoxic waters was largely contributed by PAB ($>0.8 \mu\text{m}$), which was about 2.3-3 folds of that by FLB ($0.2-0.8 \mu\text{m}$).

The bulk bacterial composition of the bottom water of X1 during the 2016 cruise with 78% of α -Proteobacteria (α -Pro), 15% of γ -Proteobacteria (γ -Pro), and 6% of Bacteroidetes was significantly different from those of X2 and X3 (91% α -Pro, 5% γ -Pro, and 2% Bacteroidetes), although their bacterial abundances were about the same (Figure 4). Compared to that of the 2016 cruise, there was a different taxonomic composition of the bulk bacterial community in the hypoxic waters of the 2019 cruise with on average 33% of α -Pro, 25% of γ -Pro, and 14% of Bacteroidetes. Furthermore, there was a substantially different taxonomic composition for PAB ($>25 \mu\text{m}$) with on average 66% of γ -Pro, 22% of α -Pro, and 4% of Bacteroidetes (Figure S2A). In particular, there was an increase of γ -Pro, but a decrease of α -Pro and Bacteroidetes, in the PAB ($>25 \mu\text{m}$) relative to the bulk bacterial community. On the genus level, the PAB ($>25 \mu\text{m}$) was largely dominated by the *Alteromonas* group in both the middle and bottom waters (Figure S2B).

3.2 PUAs concentrations in the hypoxic zone

Generally, there were significantly higher pPUAs of 0.18 nmol L^{-1} ($t=3.20$, $n=10$, $p<0.01$) and dPUAs of 0.12 nmol L^{-1} ($t=7.61$, $n=8$, $p<0.01$) in the hypoxic waters than in the nearby bottom waters without hypoxia (0.02 nmol L^{-1} and 0.01 nmol L^{-1}). Vertical distributions of pPUAs and dPUAs in the bulk seawater were showed for two stations (Y1 and Y2) inside and outside the hypoxic zone (Figure 1). Nanomolar levels of pPUAs and dPUAs were found in the water column in both stations (Figures 5E, 5F). There were high pPUAs and dPUAs in the bottom hypoxic waters of station Y1 (Figure 5E, 5F) together with locally elevated turbidity (Figure 3B) when compared to the bottom waters outside, which likely a result of particle resuspension. For station Y2 outside the hypoxia, we found negligible pPUAs and dPUAs at depths below the mixed layer (Figure 5E, 5F), which could be due to PUAs dilution by the intruded subsurface seawater.

357 Particle-adsorbed PUAs in the low-oxygen waters were quantified for the first time with the direct
358 particle volume estimated by large-volume-filtration (see the method section), which would reduce the
359 uncertainty associated with particle volume calculated by empirical equations derived for marine-snow
360 particles (Edward et al., 2015). We found high levels of particle-adsorbed PUAs ($\sim 10 \mu\text{mol L}^{-1}$) in these
361 waters (Figure 6), which were orders of magnitude higher than the bulk water pPUAs or dPUAs
362 concentrations ($< 0.3 \text{ nmol L}^{-1}$, Figure 5E, 5F). Particle-adsorbed PUAs of the low-oxygen waters mainly
363 consisted of heptadienal (C7_PUA) and octadienal (C8_PUA).

364

365 **3.3 Particle-attached bacterial growth and metabolism in the hypoxic zone**

366 Incubation of the PAB acquired from the low-oxygen waters with direct additions of different doses of
367 exogenous PUAs over 12 hours was carried out to examine the change of bacterial growth and metabolism
368 activities in response to PUA-enrichments. At the end of the incubation experiments, BA was not different
369 from the control for the PH treatment (Figure 7A). However, for the PL treatment, there were substantial
370 increases of BA in both the middle and the bottom waters compared to the initial conditions (Figure 7A). In
371 particular, BA of $\sim 3.2 \pm 0.04 \times 10^9 \text{ cells L}^{-1}$ in the bottom water for the PL treatment was significantly
372 higher ($t=12.26, n=12, p<0.01$) than the control of $2.5 \pm 0.07 \times 10^9 \text{ cells L}^{-1}$.

373 BR was significantly promoted by the low-dose PUAs with a 21.6% increase in the middle layer
374 ($t=11.91, n=8, p<0.01$) and a 25.8% increase in the bottom layer ($t=11.50, n=8, p<0.01$) compared to the
375 controls. Stimulating effect of high-dose PUAs on BR was even stronger with 47.0% increase in the middle
376 layer ($t=30.56, n=8, p<0.01$) and 39.8% increase in the bottom layer ($t=9.40, n=8, p<0.01$) (Figure 7B).
377 Meanwhile, the cell-specific BR was significantly improved for both layers with high-dose of PUAs
378 ($t=15.13, n=8, p<0.01$ and $t=4.77, n=8, p<0.01$), but not with low-dose of PUAs (Figure 7C) due to
379 increase of BA (Figure 7A). BGE was generally very low ($< 1.5\%$) during all the experiments (Figure 7D)
380 due to substantially high rates of BR (Figure 7B) than BP (Figure 7E). Also, there was no significant
381 difference in BGE between controls and PUAs treatments for both layers (Figure 7D).

382 For the bottom layer, BP was $12.6 \pm 0.8 \mu\text{g C L}^{-1} \text{d}^{-1}$ for low-dose PUAs and $16.4 \pm 0.6 \mu\text{g C L}^{-1} \text{d}^{-1}$
383 for high-dose PUAs, which were both significantly ($t=2.98, n=8, p<0.05$ and $t=10.41, n=8, p<0.01$) higher
384 than the control of $10.6 \pm 0.6 \mu\text{g C L}^{-1} \text{d}^{-1}$. Meanwhile, BP in the middle layer was significantly higher
385 ($t=2.52, n=8, p<0.05$) than the control for high-dose PUAs ($13.4 \pm 0.9 \mu\text{g C L}^{-1} \text{d}^{-1}$) but not for low-dose
386 PUAs ($12.6 \pm 0.9 \mu\text{g C L}^{-1} \text{d}^{-1}$) (Figure 7E). The cell-specific BP (sBP, 7.9 ± 0.5 and $6.9 \pm 0.2 \text{fg C cell}^{-1} \text{d}^{-1}$)
387 for high-dose PUAs were significantly ($t=2.62, n=8, p<0.05$ and $t=11.26, n=8, p<0.01$) higher than the
388 control in both layers (Figure 7F). Meanwhile, for low-dose PUAs, the sBP in both layers were not
389 significantly different from the controls.

390

391 **3.4 Particle-attached bacterial community change during incubations**

392 Generally, γ -Pro dominated (>68%) the bacterial community at the class level for all experiments, followed
393 by the second largest bacterial group of α -Pro. There was a significant increase of γ -Pro by high-dose PUAs
394 with increments of 17.2% ($t=9.25, n=8, p<0.01$) and 19.5% ($t=6.32, n=8, p<0.01$) for the middle and the
395 bottom layers, respectively (Figure 8A). However, there was no substantial change of bacterial community
396 composition by low-dose PUAs for both layers (Figure 8A).

397 On the genus level, there was also a large difference in the responses of various bacterial subgroups to
398 the exposure of PUAs (Figure 8B). The main contributing genus for the promotion effect by high-dose
399 PUAs was the group of *Alteromonas* spp., which showed a large increase in abundance by 73.9% and
400 69.7% in the middle and the bottom layers. For low-dose PUAs, the promotion effect of PUAs on
401 *Alteromonas* spp. was still found although with a much lower intensity (5.4% in the middle and 19.4% in
402 the bottom). The promotion effect of γ -Pro by high-dose PUAs was also contributed by bacteria *Halomonas*
403 spp. (percentage increase from 1.7% to 7.4%). Meanwhile, some bacterial genus, such as *Marinobacter* and
404 *Methylophaga* from γ -Pro, or *Nautella* and *Sulfitobacter* from α -Pro, showed decreased percentages by
405 high-dose PUAs (Figure 8B).

406

407 **3. 5 Carbon source preclusion experiments for PUAs**

408 After one month of incubation, PAB inoculated from the low-oxygen waters showed dramatic responses to
409 both PAH and ALK (Figure 9). In particular, the mediums of PAH addition became turbid brown (bottles on
410 the left) with the medium of ALK addition turning into milky white (bottles in the middle) (Figures 9B and
411 9D). For comparison, they were both clear and transparent at the beginning of the experiments (Figures 9A
412 and 9C). These results should reflect the growth of bacteria in these bottles with the enrichments of organic
413 carbons. Meanwhile, the minimal medium with the addition of heptadienal (C7_PUA) remained clear and
414 transparent as it was originally, which would indicate that PAB did not grow in the treatment of C7_PUA.

415

416 **4. Discussion**

417 Hypoxia occurs if the rate of oxygen consumption exceeds that of oxygen replenishment by diffusion,
418 mixing, and advection (Rabouille et al., 2008). The spatial mismatch between the surface chlorophyll-*a*
419 maxima and the subsurface hypoxia during our estuary-to-shelf transect should indicate that the
420 low-oxygen feature may not be directly connected to particle export by the surface phytoplankton bloom.
421 This outcome can be a combined result of riverine nutrient input in the surface, water-column stability
422 driven by wind and buoyancy forcing, and flow convergence for an accumulation of organic matters in the
423 bottom (Lu et al., 2018).

424 Elevated concentrations of pPUAs and dPUAs near the bottom boundary of the salt-wedge should
425 reflect a sediment source of PUAs, as the surface phytoplankton above them was very low. PUA-precursors
426 such as PUFA could be accumulated as detritus in the surface sediment near the PRE mouth during the
427 spring blooms (Hu et al., 2006). Strong convergence at the bottom of the salt-wedge could be driven by
428 shear vorticity and topography (Lu et al., 2018). This would allow for the resuspension of small detrital
429 particles. Improved PUAs production by oxidation of the resuspended PUFA could occur below the
430 salt-wedge as a result of enhanced lipoxygenase activity (in the resuspended organic detritus) in response to
431 salinity increase by the intruded bottom seawater (Galeron et al., 2018).

432 Direct measurement of the adsorbed PUAs concentration associated with the suspended particles
433 of $>25\ \mu\text{m}$ by the method of combined large-volume filtration and on-site derivation and extraction yield a
434 high level of $\sim 10\ \mu\text{mol L}^{-1}$ within the hypoxic zone. This value is comparable to those previously reported
435 in sinking particles ($>50\ \mu\text{m}$) of the open ocean using particle-volume calculated from diatom-derived
436 marine snow particles (Edward et al., 2015). Note that there was also a higher level of $240\ \mu\text{mol L}^{-1}$ found
437 in another station outside the PRE. A micromolar level of particle-adsorbed PUAs could act as a hotspot for
438 bacteria likely exerting important impacts as signaling molecules on microbial utilization of particulate
439 organic matters and subsequent oxygen consumption.

440 It should be mentioned that various pore sizes have been used for separating PAB sampling in the
441 literature. A $0.8\text{-}\mu\text{m}$ filtration was generally accepted for separating PAB ($>0.8\ \mu\text{m}$) and FLB ($0.2\text{-}0.8\ \mu\text{m}$)
442 in the ocean (Robinson and Williams, 2005; Kirchman, 2008; Huang et al., 2018; Liu et al., 2020). Other
443 studies defined size of $>3\ \mu\text{m}$ for PAB and $0.2\text{-}3\ \mu\text{m}$ for FLB in some coastal waters (Crump et al. 1999;
444 Garneau et al., 2009; Zhang et al., 2016). Meanwhile, there were also many studies using much larger sizes
445 of filtration for PAB: a $5\text{-}\mu\text{m}$ filter in the German Wadden Sea (Rink et al. 2003), a $10\text{-}\mu\text{m}$ filter in the Santa
446 Barbara Channel (DeLong et al. 1993), a $30\text{-}\mu\text{m}$ filter in the Black Sea (Fuchsman et al., 2011), and a
447 $50\text{-}\mu\text{m}$ -mesh nylon net in the North Atlantic waters (Edwards et al., 2015).

448 The hypoxic waters below the salt-wedge have high turbidity probably due to particle resuspension.
449 High particle concentration here may explain the pervious finding of a higher abundance of PAB than FLB
450 in the same area (e.g. Li et al., 2018; Liu et al., 2020), similar to those found in the Columbia River estuary
451 (Crump et al., 1998). Also, anaerobic bacteria and taxa preferring low-oxygen conditions were found more
452 enriched in the particle-attached communities than their free-living counterparts in the PRE (Zhang et al.,
453 2016). Our field measurements suggested that bacterial respiration within the hypoxic waters was largely
454 contributed by PAB ($>0.8\ \mu\text{m}$) with FLB ($0.2\text{-}0.8\ \mu\text{m}$) playing a relatively small role. Therefore, it is
455 crucial to address the linkage between the high-density PAB and the high level of particle-adsorbed PUAs
456 associated with the suspended particles in the low-oxygen waters.

457 We choose a larger pore-size of 25 μm for collecting bacteria attached to sinking aggregates and large
458 suspended particles. Firstly, it has been suggested that microbial respiration rate can be positively related to
459 aggregate size (Ploug et al., 2002) and thus larger PAB likely contributes more to oxygen consumption.
460 Secondly, larger particle size can better present the PAB taxonomy according to the previous finding of the
461 saturation of species-accumulation (for the size-fractionated bacteria) when the size is greater than 20 μm
462 (Mestre et al., 2017). Thus, the taxonomic groups of PAB caught on particles of $>25 \mu\text{m}$ should already
463 cover those of PAB on smaller particles of 0.8-25 μm . A similar type of filtration (30 μm) has been
464 previously applied to study PAB in the Black Sea suboxic zones (Fuchsman et al., 2011).

465 Interestingly, our PUA-amended experiments for PAB ($>25 \mu\text{m}$) retrieved from the low-oxygen waters
466 revealed distinct responses of PAB to different doses of PUAs treatments with an increase in cell growth in
467 response to low-dose PUAs ($1 \mu\text{mol L}^{-1}$) but an elevated cell-specific metabolic activity including bacterial
468 respiration and production in response to high-dose PUAs ($100 \mu\text{mol L}^{-1}$). An increase in cell density of
469 PAB by low-dose PUAs could likely reflect the stimulating effect of PUAs on PAB growth. This finding
470 was consistent with the previous report of a PUAs level of 0-10 $\mu\text{mol L}^{-1}$ stimulating respiration and cell
471 growth of PAB in sinking particles of the open ocean (Edwards et al., 2015). The negligible effect of
472 low-dose PUAs on bacterial community structure in our experiments was also in good agreement with
473 those found for PAB from sinking particles (Edwards et al., 2015). However, we do not see the inhibitory
474 effect of $100 \mu\text{mol L}^{-1}$ PUAs on PAB respiration and production previously found in the open ocean
475 (Edward et al., 2015). Instead, the stimulating effect for high-dose PUAs on bacterial respiration and
476 production was even stronger with $\sim 50\%$ increments. The bioactivity of PUAs on bacterial strains could
477 likely arise from its specific arrangement of two double bonds and carbonyl chain (Ribalet et al., 2008).
478 Our findings support the important role of PUAs in enhancing bacterial oxygen utilization in low-oxygen
479 waters.

480 It should be mentioned that it remains controversial the effect of background nanomolar PUAs on
481 free-living bacteria, which is not our focus in this study. Previous studies suggested that 7.5 nmol L^{-1} PUAs

482 would have a different effect on the metabolic activities of distinct bacterial groups in the NW
483 Mediterranean Sea, although bulk bacterial abundance remained unchanged (Balestra et al., 2011). In
484 particular, the metabolic activity of γ -Pro was least affected by nanomolar PUAs, although those of
485 Bacteroidetes and Rhodobacteraceae were markedly depressed (Balestra et al., 2011). Meanwhile, the daily
486 addition of 1 nmol L⁻¹ PUAs was found to not affect the bacterial abundance and community composition
487 during a mesocosm experiment in the Bothnian Sea (Paul et al., 2012).

488 It is important to verify that the PUAs are not an organic carbon source but a stimulator for PAB
489 growth and metabolism. This was supported by the fact that the inoculated PAB could not grow in the
490 medium with 200 μ mol L⁻¹ of PUAs although they grew pretty well in the mediums with a similar amount
491 of ALK or PAH. Our results support the previous findings that the density of *Alteromonas hispanica* was
492 not significantly affected by 100 μ mol L⁻¹ of PUAs in the minimal medium (without any organic carbons)
493 during laboratory experiments (Figure 9E), where PUAs were considered to act as cofactors for bacterial
494 growth (Ribalet et al., 2008).

495 Improved cell-specific metabolism of PAB in response to high-dose PUAs was accompanied by a
496 significant shift of bacterial community structure. The group of PAB with the greatest positive responses to
497 exogenous PUAs was genus *Alteromonas* within the γ -Pro, which is well-known to have a particle-attached
498 lifestyle with rapid growth response to organic matters (Ivars-Martinez et al., 2008). This result is
499 contradicted by the previous finding of a reduced percentage of the γ -Pro class by high-dose PUAs in the
500 PAB of open ocean sinking particles (Edward et al., 2015). Meanwhile, previous studies suggested that
501 different genus groups within the γ -Pro may respond distinctly to PUAs (Ribalet et al., 2008). Our result
502 was well consistent with the previous finding of the significant promotion effect of 13 or 106 μ mol L⁻¹
503 PUAs on *Alteromonas hispanica* from the pure culture experiment (Ribalet et al., 2008). An increase of
504 PUAs could thus confer some of the γ -Pro (mainly special species within the genus *Alteromonas*, such as *A.*
505 *hispanica*, Figure S2B) a competitive advantage over other bacteria, leading to their population dominance
506 on particles in the low-oxygen waters. These results provide evidences for a previous hypothesis that PUAs

507 could shape the bacterioplankton community composition by driving the metabolic activity of bacteria with
508 neutral, positive, or negative responses (Balestra et al., 2011).

509 The taxonomic composition of PAB (>25 μm) was substantially different from that of the bulk
510 bacteria community in the hypoxic zone (with a large increase of γ -Pro associated with particles, Figure
511 S2A). This result supports the previous report of γ -Pro being the most dominant clades attached to sinking
512 particles in the ocean (DeLong et al., 1993). A broad range of species associated with γ -Pro was known to
513 be important for quorum sensing processes due to their high population density (Doberva et al., 2015)
514 associated with sinking or suspended aggregates (Krupke et al., 2016). In particular, the genus of γ -Pro such
515 as *Alteromonas* and *Pseudomonas*, are well-known quorum-sensing bacteria that can rely on diverse
516 signaling molecules to affect particle-associated bacterial communities by coordinating gene expression
517 within the bacterial populations (Long et al., 2003; Fletcher et al., 2007).

518 It has been reported that the growths of some bacterial strains of the γ -Pro such as *Alteromonas* spp.
519 and *Pseudomonas* spp. could be stimulated and regulated by oxylipins like PUAs (Ribalet et al., 2008; Pepi
520 et al., 2017). Oxylipins were found to promote biofilm formation of *Pseudomonas* spp. (Martinez et al.,
521 2016) and could serve as signaling molecules mediating cell-to-cell communication of *Pseudomonas* spp.
522 by an oxylipin-dependent quorum sensing system (Martinez et al., 2019). As PUAs are an important group
523 of chemical cues belonging to oxylipins (Franzè et al., 2018), it is thus reasonable to expect that PUAs may
524 also participate as potential signaling molecules for the quorum sensing among a high-density *Alteromonas*
525 or *Pseudomonas*. A high level of particle-adsorbed PUAs occurring on organic particles in the low-oxygen
526 water would likely allow particle specialists such as *Alteromonas* to regulate bacterial community structure,
527 which could alter species richness and diversity of PAB as well as their metabolic functions such as
528 respiration and production when interacting with particulate organic matter in the hypoxic zone. Various
529 bacterial assemblages may have different rates and efficiencies of particulate organic matter degradation
530 (Ebrahimi et al., 2019). Coordination amongst these PAB could be critical in their ability to thrive on the
531 recycling of POC (Krupke et al., 2016) and thus likely contribute to the acceleration of oxygen utilizations

532 in the hypoxic zone. Nevertheless, the molecular mechanism of the potential PUA-dependent quorum
533 sensing of PAB may be an important topic for future study.

534 Our findings may likely apply to other coastal systems where there are large river inputs, intense
535 phytoplankton blooms driven by eutrophication, and strong hypoxia, such as the Chesapeake Bay, the
536 Adriatic Sea, and the Baltic Sea. For example, Chesapeake Bay is largely influenced by river runoff with
537 strong eutrophication-driven hypoxia during the summer as a result of increased water stratification (Fennel
538 and Testa, 2019) and enhanced microbial respiration fueled by organic carbons produced during spring
539 diatom blooms (Harding et al., 2015). Similar to the PRE, there was also a high abundance of γ -Pro in the
540 low-oxygen waters of the Chesapeake Bay associated with the respiration of resuspended organic carbon
541 (Crump et al., 2007). Eutrophication causes intense phytoplankton blooms in the coastal ocean.
542 Sedimentation of the phytoplankton carbons will lead to their accumulation in the surficial sediment
543 (Cloern, 2001), including PUFA compounds derived from the lipid production. Resuspension and oxidation
544 of these PUFA-rich organic particles during summer salt-wedge intrusion might lead to high
545 particle-adsorbed PUAs in the water column. These PUAs could likely shift the particle-attached bacterial
546 community to consume more oxygen when degrading particulate organic matter and thus potentially
547 contribute to the formation of seasonal hypoxia. In this sense, the possible role of PUAs on coastal hypoxia
548 may be a byproduct of eutrophication driven by anthropogenic nutrient loading. Further studies are required
549 to quantify the contributions from PUAs-mediated oxygen loss by aerobic respiration to total
550 deoxygenation in the coastal ocean.

551

552 **5. Conclusions**

553 In summary, we found elevated concentrations of pPUAs and dPUAs in the hypoxic waters below the
554 salt-wedge. We also found high particle-adsorbed PUAs associated with particles of $>25\ \mu\text{m}$ in the hypoxic
555 waters based on the large-volume filtration method, which could generate a hotspot PUAs concentration
556 of $>10\ \mu\text{mol L}^{-1}$ in the water column. In the hypoxic waters, bacterial respiration was largely controlled by

557 PAB (>0.8 μm) with FLB (0.2-0.8 μm) only accounting for 25-30% of the total respiration. Field
558 PUA-amended experiments were conducted for PAB associated with particles of >25 μm retrieved from the
559 low-oxygen waters. We found distinct responses of PAB (>25 μm) to different doses of PUAs treatments
560 with an increase of cell growth in response to low-dose PUAs (1 $\mu\text{mol L}^{-1}$) but an elevated cell-specific
561 metabolic activity including bacterial respiration and production in response to high-dose PUAs (100 μmol
562 L^{-1}). Improved cell-specific metabolism of PAB in response to high-dose PUAs was also accompanied by a
563 substantial shift of bacterial community structure with increased dominance of genus *Alteromonas* within
564 the γ -Pro.

565 Based on these observations, we hypothesize that PUAs may potentially act as signaling molecules for
566 coordination among the high-density PAB below the salt-wedge, which would likely allow bacteria such as
567 *Alteromonas* to thrive in degrading particulate organic matters. Very possibly, this process by changing
568 community compositions and metabolic rates of PAB would lead to an increase of microbial oxygen
569 utilization that might eventually contribute to the formation of coastal hypoxia.

570
571 *Data availability.* Some of the data used in the present study are available in the Supplement. Other data
572 analyzed in this article are tabulated herein. For any additional data please request from the corresponding
573 author.

574
575 *Supplement.* The supplement related to this article is available online at: [bg-2020-243-supplement](#).

576
577 *Author Contributions.* Q.P.L designed the project. Z.W. performed the experiments. Q.P.L and Z.W. wrote
578 the paper with inputs from all co-authors. All authors have given approval to the final version of the
579 manuscript.

580
581 *Competing interests.* The authors declare no competing financial interest.

582

583 *Acknowledgements.* We are grateful to the captains and the staff of *R/V Haike68* and *R/V Tan Kah Kee* for
584 help during the cruises. We thank Profs Dongxiao Wang (SCSIO) and Xin Liu (XMU) for organizing the
585 cruises, Mr. Yuchen Zhang (XMU) for field assistances, Profs Changsheng Zhang (SCSIO) and Weimin
586 Zhang (GIM) for analytical assistance, as well as Prof. Dennis Hansell (RSMAS) for critical comments.

587

588 *Financial support.* This work was supported by the National Natural Science Foundation of China
589 (41706181, 41676108), the National Key Research and Development Program of China
590 (2016YFA0601203), and the Key Special Project for Introduced Talents Team of Southern Marine Science
591 and Engineering Guangdong Laboratory (Guangzhou) (GML2019ZD0305). ZW also wants to
592 acknowledge a visiting fellowship (MELRS1936) from the State of Key Laboratory of Marine
593 Environmental Science (Xiamen University).

594 **REFERENCE**

- 595 Balestra, C., Alonso-Saez, L., Gasol, J. M., and Casotti, R.: Group-specific effects on coastal bacterioplankton of
596 polyunsaturated aldehydes produced by diatoms, *Aquat. Microb. Ecol.*, 63, 123-131,
597 <http://doi.org/10.3354/ame01486>, 2011.
- 598 Bartual, A., Morillo-Garcia, S., Ortega, M. J., and Cozar, A.: First report on vertical distribution of dissolved
599 polyunsaturated aldehydes in marine coastal waters, *Mar. Chem.*, 204, 1-10.
600 <https://doi.org/10.1016/j.marchem.2018.05.004>, 2018.
- 601 Breitburg, D., Levin, L. A., Oschlies, A., Gregoire, M., Chavez, F. P., Conley, D. J., Garcon, V., Gilbert, D., Gutierrez,
602 D., Isensee, K., Jacinto, G. S., Limburg, K. E., Montes, I., Naqvi, S. W. A., Pitcher, G. C., Rabalais, N. N.,
603 Roman, M. R., Rose, K. A., Seibel, B. A., Telszewski, M., Yasuhara, M., and Zhang, J.: Declining oxygen in the
604 global ocean and coastal waters, *Science*, 359, eaam7240, <http://doi.org/10.1126/science.aam7240>, 2018.
- 605 Cloern, J. E.: Our evolving conceptual model of the coastal eutrophication problem, *Mar. Ecol. Prog. Ser.*, 210:
606 223-253, <http://doi.org/10.3354/meps210223>, 2001.
- 607 Crump, B. C., Peranteau, C., Beckingham, B., and Cornwell J. C.: Respiratory succession and community succession
608 of bacterioplankton in seasonally anoxic estuarine waters, *Appl. Environ. Microb.*, 73, 6802-6810,
609 <http://doi.org/10.1128/aem.00648-07>, 2007.
- 610 Crump, B. C., Baross, J. A., and Simenstad, C. A.: Dominance of particle-attached bacteria in the Columbia River
611 estuary, USA. *Aquat. Microb. Ecol.*, 14, 7-18, <http://doi.org/10.3354/ame014007>, 1998.
- 612 Decho, A.W., Visscher, P.T., Ferry, J., et al.: Autoinducers extracted from microbial mats reveal a surprising diversity
613 of N-acylhomoserine lactones (AHLs) and abundance changes that may relate to diel pH. *Environ. Microb.*, 11:
614 409-420, <https://doi.org/10.1111/j.1462-2920.2008.01780.x>, 2009
- 615 Delong, E. F., Franks, D. G., and Alldredge, A. L.: Phylogenetic diversity of aggregate-attached vs free-living marine
616 bacterial assemblages, *Limnol. Oceanogr.* 38: 924-934, <http://doi.org/10.4319/lo.1993.38.5.0924>, 1993.
- 617 Diaz, R. J., and Rosenberg, R.: Spreading dead zones and consequences for marine ecosystems, *Science*, 321,
618 926-929, <http://doi.org/10.1126/science.1156401>, 2008.
- 619 Doberva, M., Sanchez-Ferandin, S., Toulza, E., Lebaron P., and Lami, R.: Diversity of quorum sensing autoinducer
620 synthases in the Global Ocean Sampling metagenomic database, *Aquat. Microb. Ecol.* 74: 107-119,
621 <http://doi.org/10.3354/ame01734>, 2015.
- 622 Doney, S. C., Ruckelshaus, M., Duffy, J. E., Barry, J. P., Chan, F., English, C. A., Galindo, H. M., Grebmeier, J. M.,
623 Hollowed, A. B., Knowlton, N., Polovina, J., Rabalais, N. N., Sydeman, W. J., and Talley, L. D.: Climate change
624 impacts on marine ecosystems, *Annu. Rev. Mar. Sci.*, 4, 11-37,
625 <http://doi.org/10.1146/annurev-marine-041911-111611>, 2012.
- 626 Dyksterhouse, S. E., Gray J. P., Herwig R. P., Lara J. C. and Staley J. T.: *Cycloclasticus pugetii* gen. nov., sp. nov., an
627 aromatic hydrocarbon-degrading bacterium from marine sediments, *Int. J. of Syst. Bacteriol.*, 45: 116-123,
628 <http://doi.org/10.1099/00207713-45-1-116>, 1995.
- 629 Edwards, B. R., Bidle, K. D., and van Mooy, B. A. S.: Dose-dependent regulation of microbial activity on sinking

630 particles by polyunsaturated aldehydes: implications for the carbon cycle, *P. Natl. Acad. Sci. USA.*, 112,
631 5909-5914, <http://doi.org/10.1073/pnas.1422664112>, 2015.

632 Ebrahimi, A., Schwartzman, J., and Cordero, O. X.: Cooperation and self-organization determine rate and efficiency
633 of particulate organic matter degradation in marine bacteria, *P. Natl. Acad. Sci. USA.*, 116, 23309-23316,
634 <http://doi.org/10.1073/pnas.1908512116>, 2019.

635 Fennel, K., and Testa, J. M.: Biogeochemical Controls on Coastal Hypoxia, *Annu. Rev. Mar. Sci.*, 11, 4.1-4.26,
636 <http://doi.org/10.1146/annurev-marine-010318-095138>, 2019.

637 Fletcher, M. P., Diggle, S. P., Crusz, S. A., Chhabra, S. R., Camara, M., and Williams, P.: A dual biosensor for
638 2-alkyl-4-quinolone quorum-sensing signal molecules, *Environ. Microbiol.*, 9: 2683-2693,
639 <http://doi.org/10.1111/j.1462-2920.2007.01380.x>, 2007.

640 Franzè, G., Pierson, J. J., Stoecker, D. K., and Lavrentyev, P. J.: Diatom-produced allelochemicals trigger trophic
641 cascades in the planktonic food web, *Limnol. Oceanogr.*, 63, 1093-1108, <http://doi.org/10.1002/lno.10756>, 2018.

642 Fuchsman, C.A., Kirkpatrick, J.B., Brazelton, W.J., Murray, J.W., and Staley, J.T.: Metabolic strategies of free-living
643 and aggregate-associated bacterial communities inferred from biologic and chemical profiles in the Black Sea
644 suboxic zone. *FEMS Microbiol Ecol*, 78: 586-603. <https://doi.org/10.1111/j.1574-6941.2011.01189.x>, 2011.

645 Galeron, M. A., Radakovitch, O., Charriere, B., Vaultier, F., Volkman, J. K., Bianchi, T. S., Ward, N. D., Medeiros, P.
646 M., Sawakuchi, H. O., Tank, S., Kerherve, P., and Rontani, J. F.: Lipoxigenase-induced autoxidative degradation
647 of terrestrial particulate organic matter in estuaries: A widespread process enhanced at high and low latitude, *Org.*
648 *Geochem.*, 115, 78-92, <http://doi.org/10.1016/j.orggeochem.2017.10.013>, 2018.

649 García-Martín, E. E., Aranguren-Gassis, M., Karl, D. M., et al.: Validation of the in vivo Iodo-Nitro-Tetrazolium
650 (INT) salt reduction method as a proxy for plankton respiration. *Front. Mar. Sci.*, 6, 220,
651 <http://doi.org/10.3389/fmars.2019.00220>, 2019

652 Garneau, M.E., Vincent, W.F., Terrado, R., and Lovejoy, C.: Importance of particle-associated bacterial heterotrophy
653 in a coastal Arctic ecosystem, *J. Marine Syst.*, 75, 185-197, <http://doi.org/10.1016/j.jmarsys.2008.09.002>, 2009.

654 Ge, Z., Wu, Z., Liu Z., Zhou, W., Dong, Y., and Li, Q. P.: Using detaching method to determine the abundance of
655 particle-attached bacteria from the Pearl River Estuary and its coupling relationship with environmental factors,
656 *Chinese J. Mar. Environ. Sci.*, <http://doi.org/10.12111/j.mes.20190065>, 2020.

657 Harding, Jr. L. W., , Adolf, J. E., Mallonee, M. E., Miller, W. D., Gallegos, C. L., Perry, E. S., Johnson, J. M., Sellner,
658 K. G., and Paerl H. W.: Climate effects on phytoplankton floral composition in Chesapeake Bay, *Estuar. Coast.*
659 *Shelf S.*, 162, 53-68, <http://doi.org/10.1016/j.ecss.2014.12.030>, 2015.

660 He, B. Dai, M., Zhai, W., Guo, X., and Wang, L.: Hypoxia in the upper reaches of the Pearl River Estuary and its
661 maintenance mechanisms: A synthesis based on multiple year observations during 2000-2008, *Mar. Chem.*, 167,
662 13-24, <http://doi.org/10.1016/j.marchem.2014.07.003>, 2014.

663 Hopkinson, C.S.: Shallow-water benthic and pelagic metabolism- evidence of heterotrophy in the nearshore Georgia
664 bight, *Mar. Biol.*, 87, 19-32, <http://doi.org/10.1007/bf00397002>, 1985.

665 Helm, K. P., Bindoff, N. L., and Church, J. A.: Observed decreases in oxygen content of the global ocean, *Geophys.*

666 Res. Lett., 38, L23602. <http://doi.org/10.1029/2011GL049513>, 2011.

667 Hmelo, L. R., Mincer, T. J., and Van Mooy, B. A. S.: Possible influence of bacterial quorum sensing on the hydrolysis
668 of sinking particulate organic carbon in marine environments, *Env. Microbiol. Rep.*, 3, 682-688,
669 <http://doi.org/10.1111/j.1758-2229.2011.00281.x>, 2011.

670 Huang, Y., Liu, X., Laws, E. A., Chen, B., Li, Y., Xie, Y., Wu, Y., Gao, K., and Huang, B.: Effects of increasing
671 atmospheric CO₂ on the marine phytoplankton and bacterial metabolism during a bloom: A coastal mesocosm
672 study, *Sci. Total Environ.*, 633, 618-629, <http://doi.org/10.1016/j.scitotenv.2018.03.222>, 2018.

673 Hu, J., Zhang H., and Peng P.: Fatty acid composition of surface sediments in the subtropical Pearl River estuary and
674 adjacent shelf, Southern China. *Estuar. Coast, Shelf S.*, 66: 346-356, <http://doi.org/10.1016/j.ecss.2005.09.009>,
675 2006.

676 Ianora, A., and Miralto, A.: Toxicogenic effects of diatoms on grazers, phytoplankton and other microbes: a review,
677 *Ecotoxicology*, 19, 493-511, <http://doi.org/10.1007/s10646-009-0434-y>, 2010.

678 Ivars-Martinez, E., Martin-Cuadrado, A. B., D'Auria, G., Mira, A., Ferriera, S., Johnson, J., et al.: Comparative
679 genomics of two ecotypes of the marine planktonic copiotroph *Alteromonas macleodii* suggests alternative
680 lifestyles associated with different kinds of particulate organic matter. *ISME, J2*, 1194–1212, 2008.

681 Kemp, W. M., Testa, J. M., Conley, D. J., Gilbert, D., and Hagy, J. D.: Temporal responses of coastal hypoxia to
682 nutrient loading and physical controls, *Biogeosciences*, 6, 2985-3008, <http://doi.org/10.5194/bg-6-2985-2009>,
683 2009.

684 Krupke, A., Hmelo, L. R., Ossolinski, J. E., Mincer, T. J., and Van Mooy, B. A. S.: Quorum sensing plays a complex
685 role in regulating the enzyme hydrolysis activity of microbes associated with sinking particles in the ocean,
686 *Front. Mar. Sci.*, 3:55, <http://doi.org/10.3389/fmars.2016.00055>, 2016.

687 Kirchman D. L.: Leucine incorporation as a measure of biomass production by heterotrophic bacteria, in: *Hand book*
688 *of methods in aquatic microbial ecology*, edited by: Kemp, P. F., Cole, J. J., Sherr, B. F., and Sherr, E. B., Lewis
689 Publishers, Boca Raton, 509–512, <http://doi.org/10.1201/9780203752746-59>, 1993.

690 Kirchman D. L.: *Microbial ecology of the oceans*, 2nd Ed., Hoboken, New Jersey, Wiley, 1-593,
691 <http://doi.org/10.1002/9780470281840>, 2008.

692 Lee, S., Lee, C., Bong, C., Narayanan, K., and Sim, E.: The dynamics of attached and free-living bacterial population
693 in tropical coastal waters, *Mar. Freshwater Res.*, 66, 701-710, <http://doi.org/10.1071/mf14123>, 2015.

694 Li, J., Salam, N., Wang, P. et al.: Discordance between resident and active bacterioplankton in free-living and
695 particle-associated communities in estuary ecosystem. *Microb. Ecol.*, 76, 637–647,
696 <https://doi.org/10.1007/s00248-018-1174-4>, 2018

697 Liu, Y., Lin, Q., Feng, J., et al.: Differences in metabolic potential between particle-associated and free-living
698 bacteria along Pearl River Estuary, *Sci. Total Environ.*, 728, 138856,
699 <https://doi.org/10.1016/j.scitotenv.2020.138856>, 2020

700 Long, R. A., Qureshi, A., Faulkner, D. J., and Azam, F.: 2-n-pentyl-4-quinolinol produced by a marine *Alteromonas*
701 sp and its potential ecological and biogeochemical roles, *Appl. Environ. Microb.*, 69, 568-576,

702 <http://doi.org/10.1128/aem.69.1.568-576.2003>, 2003.

703 Lu, Z., Gan, J., Dai, M., Liu, H., and Zhao, X.: Joint effects of extrinsic biophysical fluxes and intrinsic
704 hydrodynamics on the formation of hypoxia west off the Pearl River Estuary, *J. Geophys. Res.-Oceans.*, 123,
705 <https://doi.org/10.1029/2018JC014199>, 2018.

706 Lunau, M., Lemke, A., Walther, K., Martens-Habbena, W., and Simon, M.: An improved method for counting
707 bacteria from sediments and turbid environments by epifluorescence microscopy, *Environ. Microbiol.*, 7,
708 961-968, <http://doi.org/10.1111/j.1462-2920.2005.00767.x>, 2005.

709 Marie, D., Partensky, F., Jacquet, S. and Vaulot, D.: Enumeration and cell cycle analysis of natural populations of
710 marine picoplankton by flow cytometry using the nucleic acid stain SYBR Green I, *Appl. Environ. Microbiol.*,
711 63, 186-193, <http://doi.org/10.1128/AEM.63.1.186-193.1997>, 1997.

712 Martinez, E., and Campos-Gomez, J.: Oxylipins produced by *Pseudomonas aeruginosa* promote biofilm formation
713 and virulence, *Nat. Commun.*, 7, 13823, <https://doi.org/10.1038/ncomms13823>, 2016.

714 Martinez, E., Cosnahan, R. K., Wu, M. S., Gadila, S. K., Quick, E. B., Mobley, J. A., and Campos-Gomez, J.:
715 Oxylipins mediate cell-to-cell communication in *Pseudomonas aeruginosa*, *Commun. Biol.*, 2, 66,
716 <https://doi.org/10.1038/s42003-019-0310-0>, 2019.

717 Mestre, M., Borrull, E., Sala, M., et al.: Patterns of bacterial diversity in the marine planktonic particulate matter
718 continuum, *ISME J.*, 11, 999-1010, <https://doi.org/10.1038/ismej.2016.166>, 2017.

719 Oudot, C., Gerard, R., Morin, P., and Gningue, I.: Precise shipboard determination of dissolved-oxygen (winkler
720 procedure) for productivity studies with a commercial system, *Limnol. Oceanogr.*, 33, 146-150,
721 <http://doi.org/10.4319/lo.1988.33.1.0146>, 1988.

722 Parsons, T. R., Maita, Y., and Lalli, C. M.: Fluorometric Determination of Chlorophylls, in: *A manual of chemical*
723 *and biological methods for seawater analysis*, Pergamum Press, Oxford, 107-109,
724 <http://doi.org/10.1016/B978-0-08-030287-4.50034-7>, 1984.

725 Paul, C., Reunamo, A., Lindehoff, E., et al.: Diatom derived polyunsaturated aldehydes do not structure the
726 planktonic microbial community in a mesocosm study, *Mar. Drugs*, 10, 775-792,
727 <http://doi.org/10.3390/md10040775>, 2012.

728 Pepi, M., Heipieper, H. J., Balestra, C., Borra, M., Biffali, E., and Casotti, R.: Toxicity of diatom polyunsaturated
729 aldehydes to marine bacterial isolates reveals their mode of action, *Chemosphere*, 177, 258-265, 2017

730 Ploug, H., Zimmermann-Timm, H., and Schweitzer, B.: Microbial communities and respiration on aggregates in the
731 Elbe Estuary, Germany, *Aquat. Microb. Ecol.*, 27:241-248, 2002

732 Pohnert, G.: Wound-activated chemical defense in unicellular planktonic algae, *Ange. Chem. Int. Edit.*, 39,
733 4352-4354. [https://doi.org/10.1002/1521-3773\(20001201\)39:23<4352::AID-ANIE4352>3.0.CO;2-U](https://doi.org/10.1002/1521-3773(20001201)39:23<4352::AID-ANIE4352>3.0.CO;2-U), 2000

734 Rabouille, C., Conley, D. J., Dai, M. H., Cai, W. J., Chen, C. T. A., Lansard, B., Green, R., Yin, K., Harrison, P. J.,
735 Dagg, M., and McKee, B.: Comparison of hypoxia among four river-dominated ocean margins: The Changjiang
736 (Yangtze), Mississippi, Pearl, and Rhone rivers, *Cont. Shelf Res.*, 28, 1527-1537,
737 <http://doi.org/10.1016/j.csr.2008.01.020>, 2008.

738 Ribalet, F., Intertaglia, L., Lebaron, P., and Casotti, R.: Differential effect of three polyunsaturated aldehydes on
739 marine bacterial isolates, *Aquat. Toxicol.*, 86, 249-255, <http://doi.org/10.1016/j.aquatox.2007.11.005>, 2008.

740 Rink, B., Lunau, M., Seeberger, S., et al.: Diversity patterns of aggregate-associated and free-living bacterial
741 communities in the German Wadden Sea, *Ber Forschungszentrum Terramare*, 12: 96–98, 2003.

742 Robinson, C., and Williams, P. J. I.: Respiration and its measurement in surface marine waters, in: *Respiration in*
743 *Aquatic Ecosystems*, edited by de Giorgio, P. A., and Williams, P. J. I., Oxford University Press, New York,
744 147-180, <http://doi.org/10.1093/acprof:oso/9780198527084.003.0009>, 2005.

745 Su, J., Dai, M., He, B., Wang, L., Gan, J., Guo, X., Zhao, H., and Yu, F.: Tracing the origin of the oxygen-consuming
746 organic matter in the hypoxic zone in a large eutrophic estuary: the lower reach of the Pearl River Estuary, China,
747 *Biogeosciences*, 14, 4085-4099, <http://doi.org/10.5194/bg-14-4085-2017>, 2017.

748 Vidoudez, C., Casotti, R., Bastianini, M., and Pohnert, G.: Quantification of dissolved and particulate polyunsaturated
749 aldehydes in the Adriatic Sea. *Mar. Drugs*, 9, 500-513, <https://doi.org/10.3390/md9040500>, 2011.

750 Wang, N., Lin, W., Chen, B., and Huang, B.: Metabolic states of the Taiwan Strait and the northern South China Sea
751 in summer 2012, *J. Trop. Oceanogr.*, 33, 61-68, <http://doi.org/doi:10.3969/j.issn.1009-5470.2014.04.008>, 2014.

752 Williams, P. J. I. and de Giorgio, P. A.: Respiration in Aquatic Ecosystems: history and background, in: *Respiration in*
753 *Aquatic Ecosystems*, edited by de Giorgio, P. A., and Williams, P. J. I., Oxford University Press, New York, 1-17,
754 <http://doi.org/10.1093/acprof:oso/9780198527084.003.0001>, 2005.

755 Wu, Z., and Li, Q. P.: Spatial distributions of polyunsaturated aldehydes and their biogeochemical implications in the
756 Pearl River Estuary and the adjacent northern South China Sea, *Prog. Oceanogr.*, 147, 1-9,
757 <http://doi.org/10.1016/j.pocean.2016.07.010>, 2016.

758 Xu, J., Li, X., Shi, Z., Li, R., and Li, Q. P.: Bacterial carbon cycling in the river plume in the northern South China
759 Sea during summer, *J. Geophys. Res.-Oceans*, 123, 8106-8121, <http://doi.org/10.1029/2018jc014277>, 2018.

760 Yin, K., Lin, Z., and Ke, Z.: Temporal and spatial distribution of dissolved oxygen in the Pearl River Estuary and
761 adjacent coastal waters, *Cont. Shelf Res.*, 24, 1935-1948, <http://doi.org/10.1016/j.csr.2004.06.017>, 2004.

762 Zhang, H., and Li, S.: Effects of physical and biochemical processes on the dissolved oxygen budget for the Pearl
763 River Estuary during summer, *J. Marine Syst.*, 79, 65-88, <http://doi.org/10.1016/j.jmarsys.2009.07.002>, 2010.

764 Zhang, Y., Xiao, W., and Jiao, N.: Linking biochemical properties of particles to particle-attached and free-living
765 bacterial community structure along the particle density gradient from freshwater to open ocean, *J. Geophys.*
766 *Res.-Bioge.*, 121, 2261-2274, <http://doi.org/10.1002/2016jg003390>, 2016.

767 **Table 1.** Summary of treatments in the experiments of exogenous PUAs additions for the low-oxygen
768 waters at station Y1 during June 2019. The PUAs solution includes heptadienal (C7_PUA), octadienal
769 (C8_PUA), and decadienal (C10_PUA) with the mole ratios of 10:1:10.
770

		Treatment
1	Control (methanol)	methanol
2	Low-dose PUAs (methanol)	2 mM PUAs in methanol
3	High-dose PUAs (methanol)	200 mM PUAs in methanol

771
772

Figures and Legends

773

774 **Figure 1:** Sampling map of the Pearl River Estuary and the adjacent northern South China Sea during (A)
775 June 17th-28th, 2016, (B) June 18st-June 2nd, 2019. Contour shows the bottom oxygen distribution with
776 white lines highlighting the levels of 93.5 $\mu\text{mol kg}^{-1}$ (oxygen-deficient zone) and 62.5 $\mu\text{mol kg}^{-1}$ (hypoxic
777 zone); dashed line in panel A is an estuary-to-shelf transect with blue dots for three stations with bacterial
778 metabolic rate measurements; diamonds in panel B are two stations with vertical pPUAs and dPUAs
779 measurements with Y1 the station for PUAs-amended experiments.

780

781 **Figure 2:** Procedure of large-volume filtration and subsequent experiments. A large volume of the
782 low-oxygen water was filtered through a 25- μm filter to obtain the particles-adsorbed PUAs and the
783 particle-attached bacteria (PAB). The carbon-source test of PUA for the inoculated PAB includes the
784 additions of PUA, alkanes (ALK), and polycyclic aromatic hydrocarbons (PAH). PUAs-amended
785 experiments for PAB include Control (CT), Low-dose (PL), and High-dose PUAs (PH). Samples in the
786 biological oxygen demand (BOD) bottles at the end of the experiment were analysed for bacterial
787 respiration (BR), abundances (BA), production (BP) as well as DNA. Note that pPUAs and dPUAs are
788 particulate and dissolved PUAs in the seawater.

789

790 **Figure 3:** Vertical distributions of (A) temperature, (B) turbidity, (C) nitrate, (D) salinity, (E) dissolved
791 oxygen, and (F) chlorophyll-*a* from the estuary to the shelf of the NSCS during June 2016. Section
792 locations are shown in Figure 1; the white line in panel D shows the area of oxygen deficiency zone (<93.5
793 $\mu\text{mol kg}^{-1}$).

794

795 **Figure 4:** Comparisons of oxygen, bulk bacterial respiration (BR) and production (BP), as well as bulk
796 bacterial abundances (BA) of α -Proteobacteria (α -Pro), γ -Proteobacteria (γ -Pro), Bacteroidetes (Bact), and
797 other bacteria for the bottom waters between stations inside (X1) and outside (X2 and X3) the hypoxic zone
798 during the 2016 cruise. Bulk bacteria community includes FLB and PAB of <20 μm . Locations of stations
799 X1, X2, X3 are showed in Figure 1A. Error bars are the standard deviations.

800

801 **Figure 5:** Vertical distributions of (A) temperature, (B) salinity, (C) dissolved oxygen (DO), (D)
802 chlorophyll-*a* (Chl-*a*), (E) particulate PUAs (pPUAs) and (F) dissolved PUAs (dPUAs) inside (Y1) and
803 outside (Y2) the hypoxic zone during June 2019. Locations of station Y1 and Y2 are shown in Figure 1.
804 Error bars are the standard deviations.

805

806 **Figure 6:** Concentrations of particle-adsorbed PUAs (in micromoles per liter particle) in the middle (12 m)
807 and the bottom (25 m) waters of station Y1 during June 2019. Three different PUA components are also
808 shown including heptadienal (C7_PUA), octadienal (C8_PUA), and decadienal (C10_PUA). Error bars are
809 the standard deviations.

810
811 **Figure 7:** Responses of particle-attached bacterial parameters including (A) bacterial abundance (BA_{particle}),
812 (B) bacterial respiration (BR_{particle}), (C) cell-specific bacterial respiration (sBR_{particle}), (D) bacterial growth
813 efficiency (BGE_{particle}), (E) bacterial production (BP_{particle}), and (F) cell-specific bacterial production
814 (sBP_{particle}) to different doses of PUAs additions at the end of the experiments for the middle (12 m) and the
815 bottom waters (25 m) at station Y1. Error bars are standard deviations. The star represents a significant
816 difference ($p < 0.05$) with PL and PH the low and high dose PUA treatments and C the control.

817
818 **Figure 8:** Variation of particle-attached bacterial community compositions on (A) the phylum level and (B)
819 the genus level in response to different doses of PUAs additions at the end of the experiments for the
820 middle and the bottom waters at station Y1. Labels PL and PH are for the low- and high-dose PUAs with
821 CT the control.

822
823 **Figure 9:** Carbon-source test of PUAs with cell culture of particle-attached bacteria inoculated from the
824 low-oxygen waters of station Y1 including the initial conditions (Day0) at the beginning of the experiments
825 as well as results after 30 days of incubations (Day30) for (A, B) the middle and (C, D) the bottom waters,
826 respectively. Bottles from left to right are the mediums (M) with the additions of polycyclic aromatic
827 hydrocarbons (M+PAH, 200 ppm), alkanes (M+ALK, 0.25 g L^{-1}), and heptadienal (M+C7_PUA, 0.2 mmol
828 L^{-1}); Note that a change of turbidity should indicate bacterial utilization of organic carbons. (E) the optical
829 density of bacterium *Alteromonas hispanica* MOLA151 growing in the minimal medium as well as in the
830 mediums with the additions of mannitol, pyruvate, and proline (M+MPP, 1% each), heptadienal
831 (M+C7_PUA, $145 \mu\text{M}$), octadienal (M+C8_PUA, $130 \mu\text{M}$), and decadienal (M+C10_PUA, $106 \mu\text{M}$). The
832 method for *A. hispanica* growth and the data in panel E are from Ribalet et al., 2008.

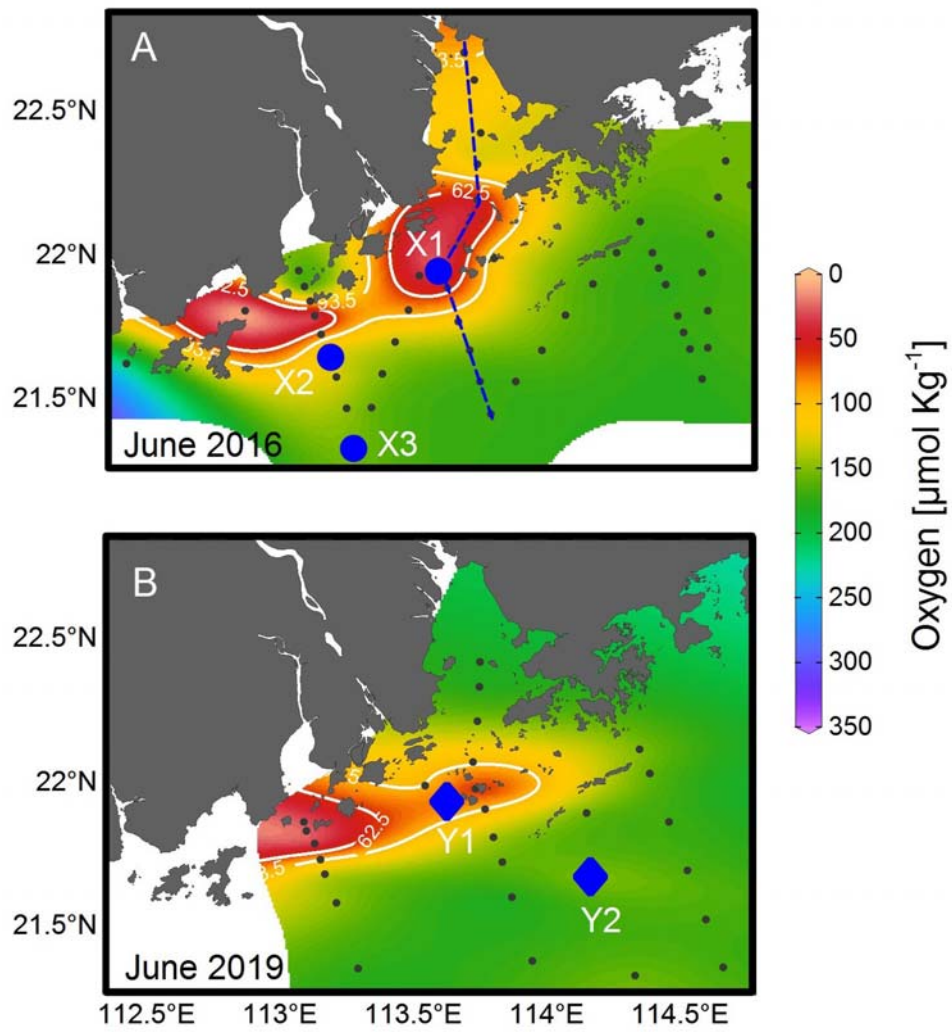


Figure 1

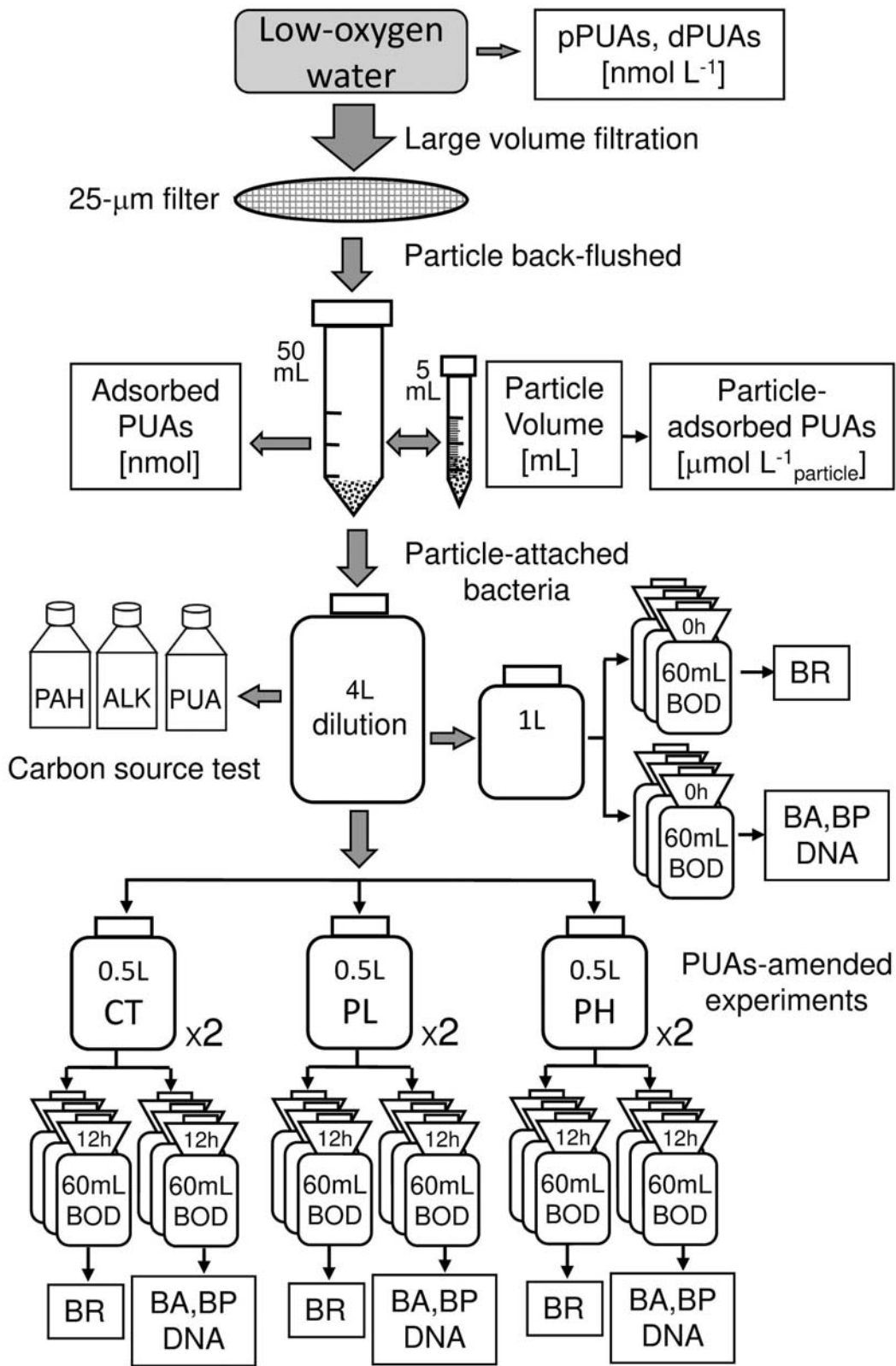
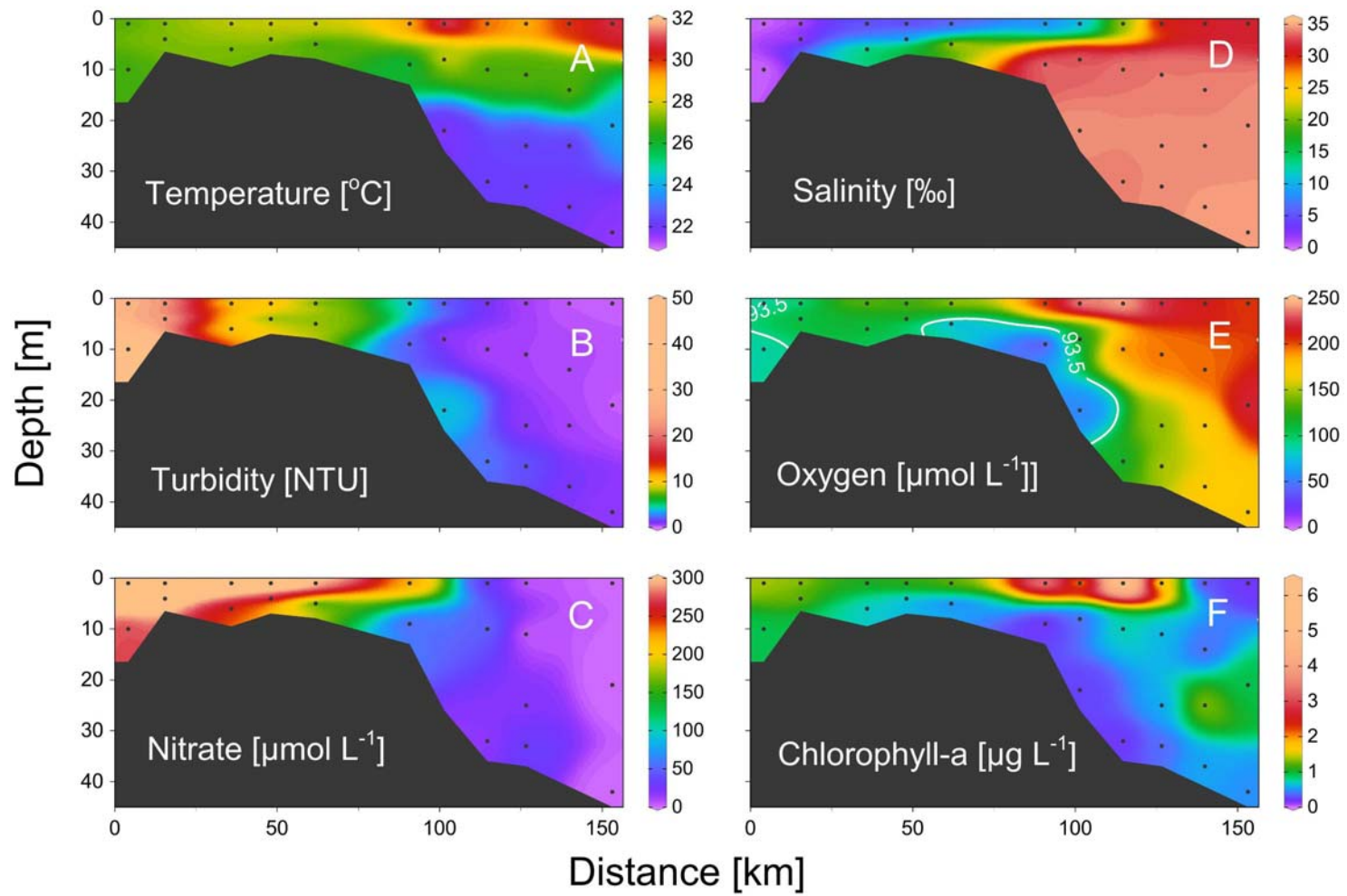


Figure 2

838

839

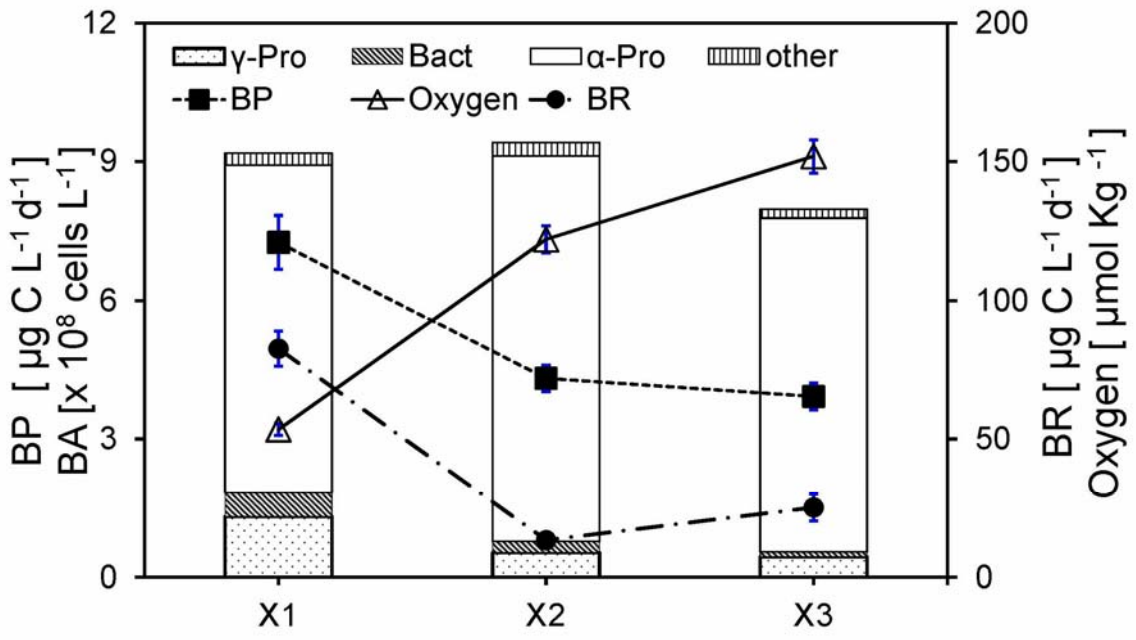


840

841

842

Figure 3



843
844
845
846

Figure 4

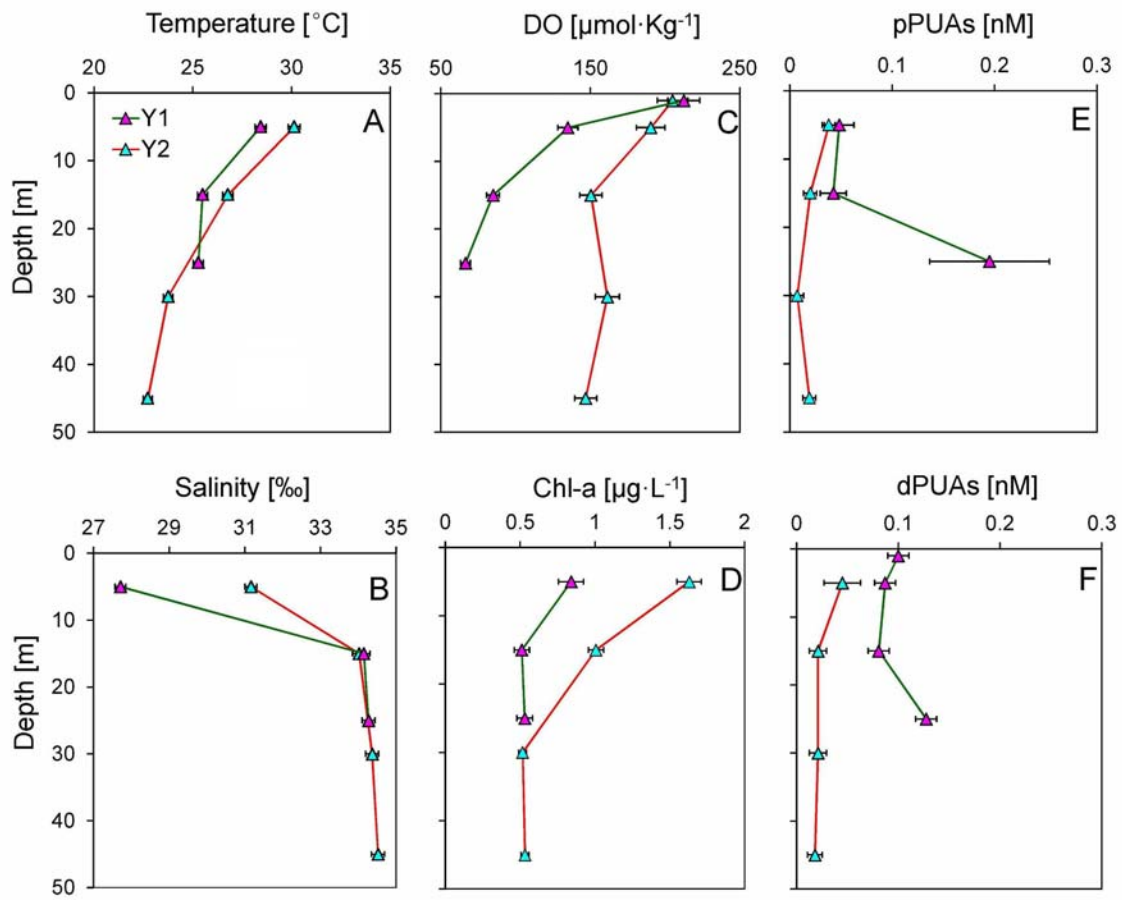


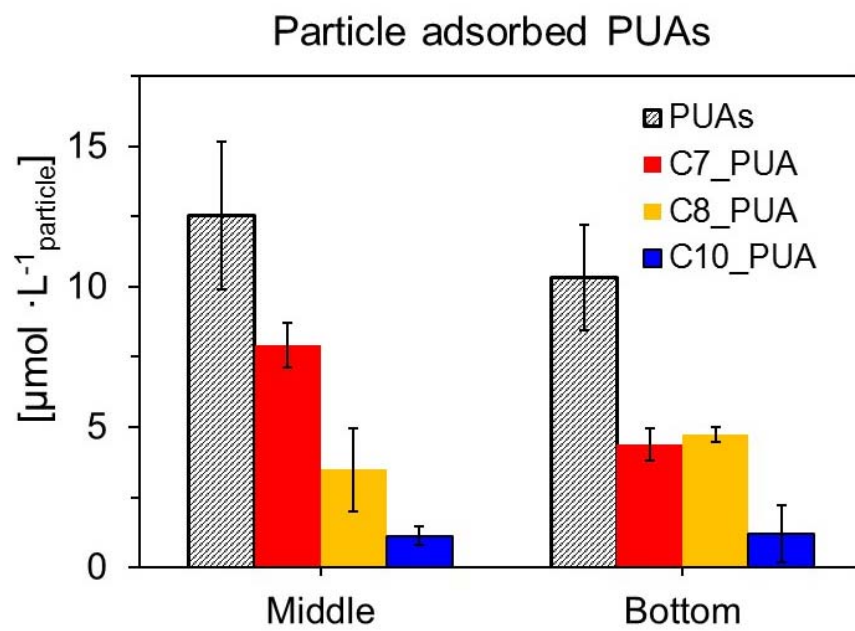
Figure 5

847

848

849

850



851
852
853
854

Figure 6

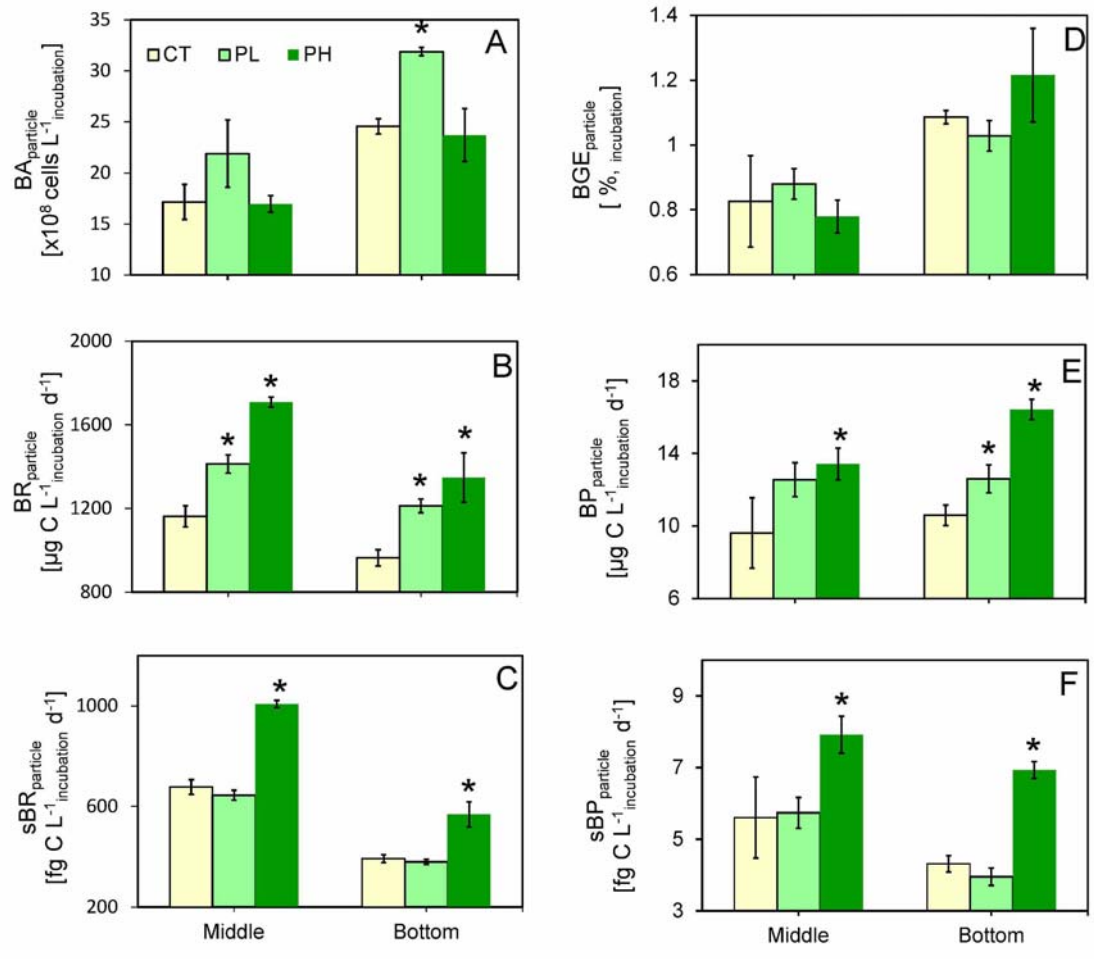


Figure 7

855
856
857
858

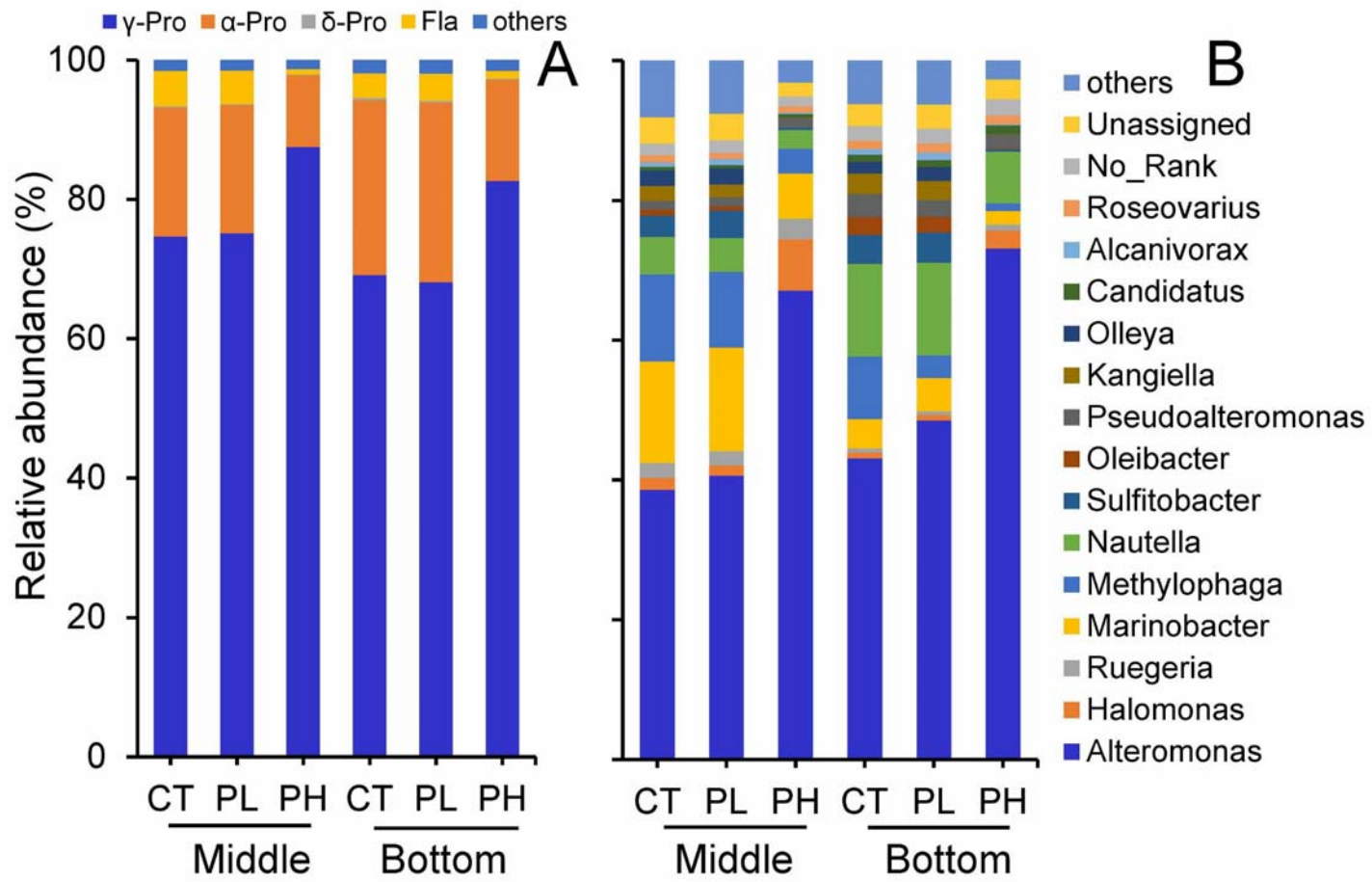
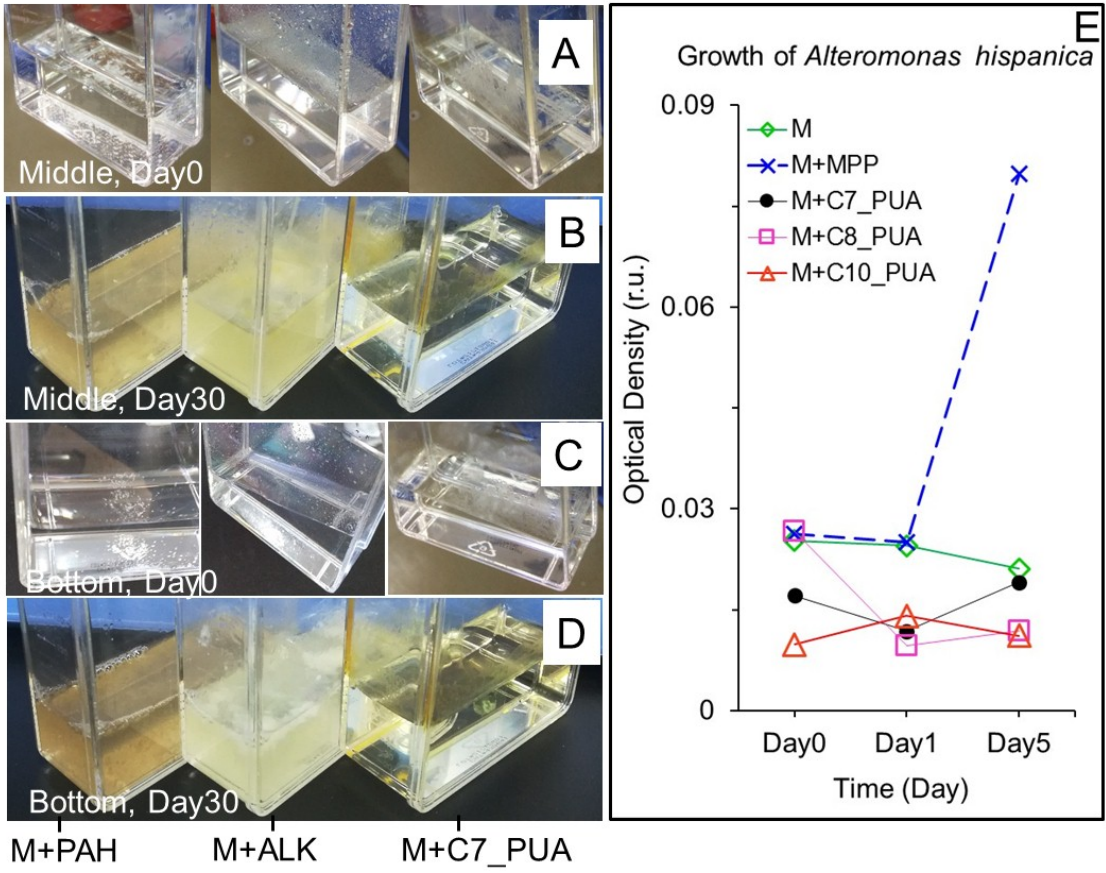


Figure 8

859

860

861



862
863
864
865

Figure 9